Arteriosclerosis, Thrombosis, and Vascular Biology

JOURNAL OF THE AMERICAN HEART ASSOCIATION

Targeted Phosphotyrosine Profiling of Glycoprotein VI Signaling Implicates Oligophrenin-1 in Platelet Filopodia Formation

Onno B. Bleijerveld, Thijs C. van Holten, Christian Preisinger, Jasper J. van der Smagt, Richard W. Farndale, Tjitske Kleefstra, Marjolein H. Willemsen, Rolf T. Urbanus, Philip G. de Groot, Albert J.R. Heck, Mark Roest and Arjen Scholten

Arterioscler Thromb Vasc Biol. 2013;33:1538-1543; originally published online April 25, 2013;
doi: 10.1161/ATVBAHA.112.300916
Arteriosclerosis, Thrombosis, and Vascular Biology is published by the American Heart Association, 7272 Greenville Avenue, Dallas, TX 75231

Print ISSN: 1079-5642. Online ISSN: 1524-4636

Targeted Phosphotyrosine Profiling of Glycoprotein VI Signaling Implicates Oligophrenin-1 in Platelet Filopodia Formation

Onno B. Bleijerveld,* Thijs C. van Holten,* Christian Preisinger, Jasper J. van der Smagt, Richard W. Farndale, Tjitske Kleefstra, Marjolein H. Willemsen, Rolf T. Urbanus, Philip G. de Groot, Albert J.R. Heck, Mark Roest, Arjen Scholten

Objective—Platelet adhesion to subendothelial collagen is dependent on the integrin $\alpha_2\beta_1$ and glycoprotein VI (GPVI) receptors. The major signaling routes in collagen-dependent platelet activation are outlined; however, crucial detailed knowledge of the actual phosphorylation events mediating them is still limited. Here, we explore phosphotyrosine signaling events downstream of GPVI with site-specific detail.

Approach and Results—Immunoprecipitations of phosphotyrosine-modified peptides from protein digests of GPVI-activated and resting human platelets were compared by stable isotope-based quantitative mass spectrometry. We surveyed 214 unique phosphotyrosine sites over 2 time points, of which 28 showed a significant increase in phosphorylation on GPVI activation. Among these was Tyr370 of oligophrenin-1 (OPHN1), a Rho GTPase–activating protein. To elucidate the function of OPHN1 in platelets, we performed an array of functional platelet analyses within a small cohort of patients with rare oligophrenia. Because of germline mutations in the *OPHN1* gene locus, these patients lack OPHN1 expression entirely and are in essence a human knockout model. Our studies revealed that among other unaltered properties, patients with oligophrenia show normal P-selectin exposure and $\alpha_{IIb}\beta_3$ activation in response to GPVI, as well as normal aggregate formation on collagen under shear conditions. Finally, the major difference in OPHN1-deficient platelets turned out to be a significantly reduced collagen-induced filopodia formation.

Conclusions—In-depth phosphotyrosine screening revealed many novel signaling recipients downstream of GPVI activation uncovering a new level of detail within this important pathway. To illustrate the strength of such data, functional follow-up of OPHN1 in human platelets deficient in this protein showed reduced filopodia formation on collagen, an important parameter of platelet hemostatic function. **(*Arterioscler Thromb Vasc Biol*. 2013;33:1538-1543.)**

Key Words: hemostasis ■ oligophrenin-1 deficiency ■ platelet GPVI signaling ■ proteomics ■ tyrosine phosphorylation

The response of platelets to vessel injury is essential to prevent bleeding, but hyperreactivity underlies the pathophysiology of various thrombotic diseases. Exposure of the extracellular matrix to flowing blood induces platelet activation, including the release of the contents of α- and δ-granules. In addition, a conformational change in $\alpha_{IIb}\beta_3$ increases its affinity for its ligands (eg, fibrinogen) and an active reorganization of the actin cytoskeleton accommodates shape change and the formation of filopodia.[1] Collagen, the most abundant matrix protein in the subendothelium, provides a primary activation stimulus and a surface for adhesion.[2] Glycoprotein VI (GPVI) is considered the predominant receptor responsible for collagen-induced platelet activation.[3,4]

The GPVI-mediated signaling pathway is a promising target for novel antiplatelet therapies because individuals with reduced GPVI expression have a mild increase in bleeding tendencies, whereas inhibition of the GPVI pathway may reduce thrombosis risk.[2,5–7] Therefore, it is important to improve our knowledge of the GPVI-mediated signaling pathway in platelet activation.

GPVI is a 62-kDa type I transmembrane receptor of the immunoglobulin superfamily of surface receptors, which

Received on: November 29, 2012; final version accepted on: April 10, 2013.

From the Biomolecular Mass Spectrometry and Proteomics and Bijvoet Center for Biomolecular Research and Utrecht Institute for Pharmaceutical Sciences, Utrecht University, Utrecht, The Netherlands (O.B.B., C.P., A.J.R.H., A.S.); Netherlands Proteomics Centre, Utrecht, The Netherlands (O.B.B., C.P., A.J.R.H., A.S.); Departments of Clinical Chemistry and Haematology (T.C.v.H., R.T.U., P.G.d.G., M.R.) and Medical Genetics (J.J.v.d.S.), University Medical Center Utrecht, Utrecht, The Netherlands; Department of Biochemistry, University of Cambridge, Cambridge, United Kingdom (R.W.F.); Department of Human Genetics, Radboud University Nijmegen Medical Centre, Nijmegen, The Netherlands (T.K., M.H.W.). O.B.B. is currently affiliated with the Laboratory of Experimental Cardiology, University Medical Center Utrecht, Utrecht, The Netherlands.

*These authors contributed equally.

The online-only Data Supplement is available with this article at http://atvb.ahajournals.org/lookup/suppl/doi:10.1161/ATVBAHA.112.300916/-/DC1.

Correspondence to Mark Roest, PhD, Department of Clinical Chemistry and Haematology, University Medical Center Utrecht, Heidelberglaan 100, 3584 CX Utrecht, The Netherlands (e-mail m.roest@umcutrecht.nl); or Arjen Scholten, PhD, Biomolecular Mass Spectrometry and Proteomics, Utrecht Institute of Pharmaceutical Science, Utrecht University, Padualaan 8, 3584 CH Utrecht, The Netherlands (e-mail a.scholten@uu.nl).

is exclusively expressed in platelets and megakaryocytes. The signaling capacity of GPVI depends on its association with the Fc receptor γ-chain homodimer. Each Fc receptor γ-chain monomer contains a conserved immunoreceptor tyrosine–based activation motif, which is characterized by 2 conserved YXXL motifs separated by 6 to 12 amino acids.[8] On receptor cross-linking by the ligand collagen these 2 conserved immunoreceptor tyrosine–based activation motif tyrosine residues are phosphorylated by the Src family tyrosine kinases, Fyn and Lyn, which localize to a conserved proline-rich region of GPVI.[3,9] This phosphorylation then leads to recruitment and activation of the tyrosine kinase Syk, which regulates a complex downstream pathway that involves the adapter proteins LAT, Gads, and SLP-76; the Tec family tyrosine kinases Btk and Tec; the GTP exchange factors Vav1 and Vav3; phosphatidylinositol 3-kinase isoforms; and phospholipase C-γ2.[9,10]

A handful of proteins that participate in GPVI signaling in human platelets are known, but our understanding of the tyrosine signaling events downstream of GPVI activation is far from complete. This information is considered crucial for understanding the fine molecular details of platelet activation and their clinical implications. Here, we aimed to identify novel GPVI signaling proteins by obtaining site-specific and quantitative information on tyrosine residues being phosphorylated on stimulation. To this end, a quantitative analysis of immunoaffinity-enriched phosphorylated tyrosine peptides[11–13] was performed to compare resting and cross-linked collagen-related peptide (CRP-XL)-stimulated human platelets.[14] We identified 214 unique phosphotyrosine (pTyr) sites of which 30 showed >2-fold increase in tyrosine phosphorylation after stimulation. Next to expected downstream targets of GPVI, we also detected 3 putatively novel ones. One of these, oligophrenin-1 (OPHN1), is a Rho GTPase–activating protein. Subsequent characterization

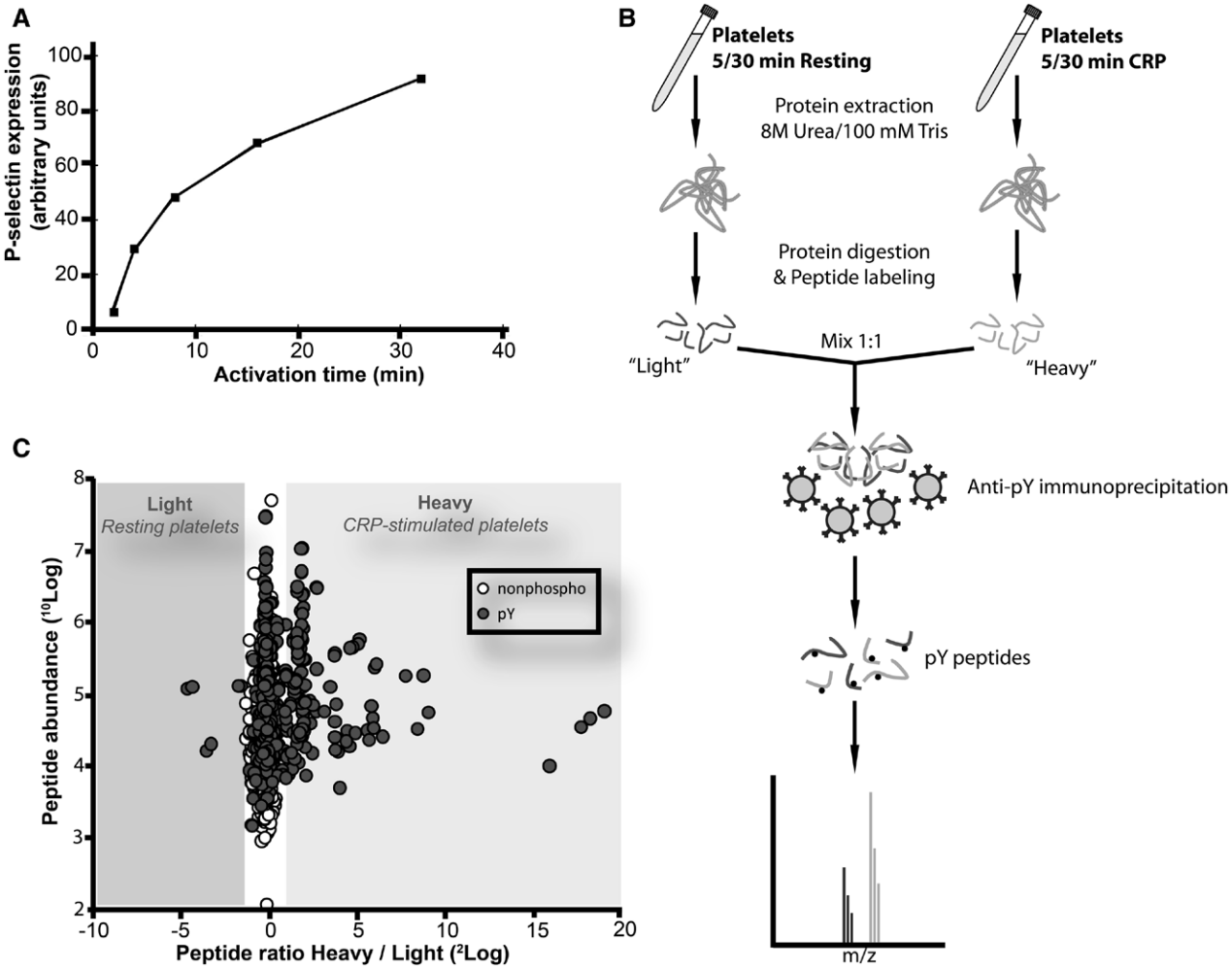

Figure 1. Targeted tyrosine phosphorylation profiling in stimulated platelets. **A**, Platelet stimulation with 2.5 μg/mL cross-linked collagen-related peptide (CRP-XL) as monitored by P-selectin expression on the plasma membrane. **B**, Overview of the experimental quantitative proteomics workflow. In parallel, resting (**left**) and CRP-XL–activated (5 and 30 minutes, **right**) platelets were lysed, proteins extracted and subsequently digested with trypsin. The peptides were differentially labeled using stable isotope dimethyl labeling. For each time point, 2 differentially labeled digests were combined, followed by enrichment of tyrosine-phosphorylated peptides using immobilized phosphotyrosine-specific antibodies. The enriched fraction was analyzed by nanoflow liquid chromatography–mass spectrometry (MS)/MS. **C**, Proteomics data representation (30-minute experiment is shown as an example). Using MSQuant software, the ratio (heavy/light)=(CRP-XL/Ctrl) was calculated for immunoprecipitated phosphotyrosine (pY)-containing peptides (dark grey dots) and normalized on the ratio of nonphosphorylated peptides (white dots), based on the extracted ion chromatograms of the differentially labeled isotopomers of each peptide. Peptide ratios (^{2}log values) were plotted against peptide abundance (intensity, ^{10}log values).

of platelets obtained from 4 patients with X-linked intellectual disability caused by germline mutations in the *OPHN1* gene (OMIM 300486) revealed the specific involvement of *OPHN1* in platelet filopodia formation on collagen, substantiating our data obtained from the targeted pTyr proteome profiling approach.

Materials and Methods

Materials and Methods are available in the online-only Supplement.

Results

Tyrosine Phosphoproteome Analysis of CRP-XL–Stimulated Platelets

Platelets need to respond rapidly to changes in vascular integrity to prevent excessive blood loss. Signaling pathways leading to platelet activation are therefore rapidly activated on stimulation. To capture most detail, optimal time points of GPVI stimulation for our in-depth targeted and quantitative analysis were evaluated on the kinetics of CRP-XL–dependent platelet activation. To this end, quantification of platelet membrane P-selectin expression, a general marker of activation, was used (Figure 1A). Two time points were selected: 5 minutes to represent the onset and 30 minutes to represent maximal activation. The chosen proteomics approach, which uses specific immune enrichment of peptides carrying a tyrosine phosphorylation is schematically depicted in Figure 1B.[11,12,15] After analysis of both the 5- and 30-minute time point, in total 214 pTyr sites on 148 proteins were identified (Table I in the online-only Data Supplement).

The quantitative data, based on stable isotope dimethyl labeling, revealed that, as expected, overall protein abundance levels (reflected in the [CRP-XL/Ctrl] ratios of nonphosphorylated peptides) remained identical when comparing resting and activated platelets at both the 5- and 30-minute time point (Figure 1C and Figure IA and IB in the online-only Data Supplement). In contrast, many tyrosine-containing peptides showed >2-fold increased phosphorylation on CRP-XL stimulation (28 unique tyrosine sites on 27 proteins), the majority being detected at both time points (Figure 2 and Figure IC in the online-only Data Supplement). Among these were several expected proteins and tyrosine phosphorylation sites belonging to the presumed core GPVI response proteome (Figure 2 and Figure II in the online-only Data Supplement): one of the Fc receptor γ-chain immunoreceptor tyrosine–based activation motif domains (FCER1G; Tyr65), SYK (Tyr629/Tyr630), GRAP2 (GADS; Tyr45), and other proteins comprising the LAT signalosome.[9] Twenty-two (80%) of the regulated tyrosine sites with increased phosphorylation on GPVI activation are novel in platelets (Figure 2, black stars), according to the Uniprot and PhosphoSitePlus human databases and several key references.[16–18] Three particular sites were present on proteins not earlier shown to be involved in platelet collagen signaling: the protein tyrosine kinase ABL1/ABL2 (Tyr393/Tyr439), the nonreceptor type protein tyrosine phosphatase 18 (Tyr389), and the Rho GTPase–activating protein OPHN1 (Tyr370).

Characterization of OPHN1-Deficient Platelets

Deficiency of OPHN1 (OPHN1$^{-/y}$) is associated with a rare form of X-linked mental retardation known as oligophrenia, a syndrome characterized by defects in neuronal dendrite formation and synaptic plasticity.[19,20] Despite the fact that oligophrenia is

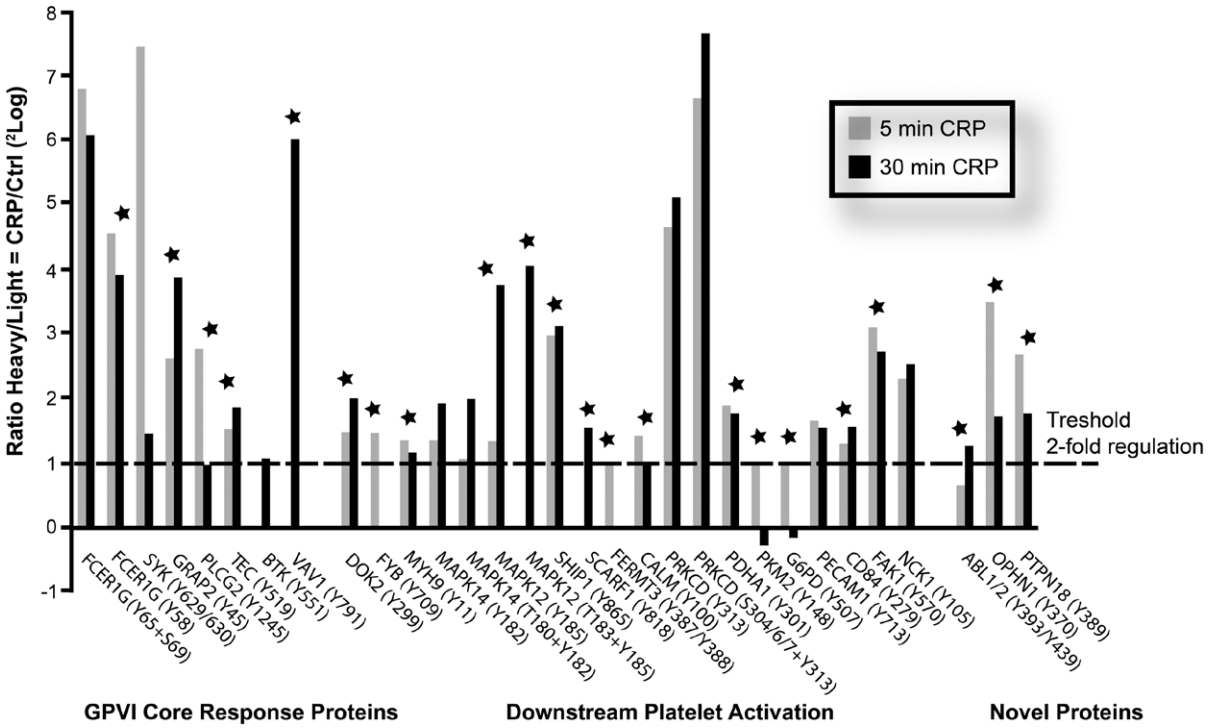

Figure 2. Tyrosine sites undergoing increased phosphorylation downstream of glycoprotein (GP)VI activation. Tyrosine phosphorylation sites with increased phosphorylation downstream of GPVI in platelets activated with cross-linked collagen-related peptide (CRP-XL). Twenty-eight phosphotyrosine (pTyr) sites on 27 proteins showed at least 2-fold increase in phosphorylation in response to platelet activation through GPVI after 5 minutes (grey bars) and 30 minutes (black bars). A substantial part of these sites belongs to the GPVI core response proteome (Figure II in the online-only Data Supplement). Novel pTyr sites in platelet activation are marked with black stars.

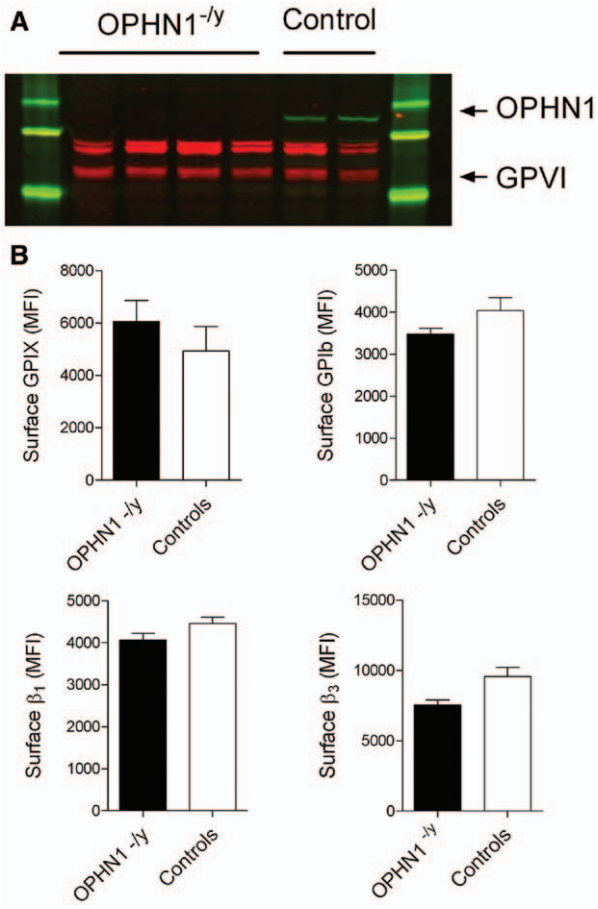

Figure 3. Expression levels of oligophrenin-1 (OPHN1) and several platelet receptors in OPHN1$^{-/y}$ patients and controls. **A**, Washed platelets from 4 OPHN1$^{-/y}$ patients and 2 healthy controls were lysed and analyzed by Western blotting using goat antioligophrenin-1 polyclonal antibody (green) and sheep anti-glycoprotein (GP) VI polyclonal antibody (red). **B**, Platelets from 4 OPHN1$^{-/y}$ patients (black bars) and 5 controls (white bars) were incubated with antibodies against β_3, α_2, GPIb, and GPIX and expression was analyzed by flow cytometry. Data are expressed as mean median relative fluorescence units (MFI)±SD.

a rare disorder, we were able to obtain blood from 4 OPHN1-deficient patients. As far as we know, no bleeding disorders are reported in relation to loss of OPHN1. In line, the patients did not have a bleeding phenotype, and there were no indications of thrombotic complications. Although each patient had a different gene variant, Western blotting confirmed the absence of OPHN1 in the platelets of each patient (Figure 3A), whereas 2 control individuals showed robust expression of OPHN1 in their isolated platelet lysates (apparent molecular mass 91 kDa). The mean platelet count±SD (434±56×10^9/L), mean platelet volume±SD (7.3±0.6 fL), and the expression of the platelet surface receptors GPIbα, GPIX, β_1-integrin, and the β_3-integrin were within the normal range in OPHN1$^{-/y}$ platelets (Figure 3B).

OPHN1-Deficient Platelets Are Hemostatically Normal

To determine whether the absence of OPHN1 affects platelet function, we assessed the response of OPHN1-deficient platelets to stimulation of $P2Y_{12}$, PAR-1, and GPVI (Figure III in the online-only Data Supplement). OPHN1-deficient platelets showed no significant differences in P-selectin expression or $\alpha_{IIb}\beta_3$ activation compared with healthy controls.

We then assessed the influence of OPHN1 on platelet adhesion to collagen under conditions of high shear flow (1600/s; Figure IV in the online-only Data Supplement) and found that OPHN1$^{-/y}$ platelets adhered and formed aggregates on a collagen-coated surface to a similar extent as healthy controls. Moreover, the absence of OPHN1 did not affect clot retraction in thrombin-stimulated platelet-rich plasma (Figure V in the online-only Data Supplement).

OPHN1-Deficient Platelets Show Defective Filopodia Formation

Because deficiency of OPHN1 is reported to be associated with decreased neuronal dendrite formation,[20,21] we looked into the role of OPHN1 in platelet spreading using real-time microscopy. Because OPHN1 phosphorylation was increased on stimulation of the collagen-dependent activation pathway, we also studied platelet spreading on a mixture of the collagen peptides that bind GPVI (CRP-XL) and $\alpha_2\beta_1$ (GFOGER).[22] CRP-XL is a potent activator of platelets and causes rapid aggregate formation. Because this obscures the spreading process, we prevented aggregate formation with 0.2 mmol/L of RGD peptide, thereby blocking $\alpha_{IIb}\beta_3$-ligand interactions. Under these conditions, OPHN1$^{-/y}$ platelets showed equal lamellipodia formation but significantly less filopodia formation during spreading (Figure 4A and 4B, Movies I and II in the online-only Data Supplement). OPHN1$^{-/y}$ platelets form filopodia (OPHN1$^{-/y}$, 100±SEM 0%; controls, 99±SEM 1%; not significant) and spread normally on fibrinogen (OPHN1$^{-/y}$, 68±SEM 11%; controls, 83±SEM 7%; not significant), which is mainly $\alpha_{IIb}\beta_3$-dependent. In addition, we did not observe differences in filopodia length between OPHN1$^{-/y}$ platelets and control platelets spreading on surfaces coated with CRP-XL and GFOGER (Figure 4C) or on fibrinogen-coated surfaces (data not shown).

Discussion

To study the nature of GPVI signaling specifically in human platelets, we used anti-pTyr immunoprecipitation of peptides, directly from primary human platelet digests. The quantitative proteomics data show immediately that GPVI signaling was rapidly engaged because of the highly increased phosphorylation of the immunoreceptor tyrosine–based activation motif domain at Tyr65 after 5 minutes. In addition, the phosphorylation of other known downstream targets was prominent (Syk, GADS, etc), confirming the validity of our approach.

García et al[16] have used pTyr immunoprecipitation at the protein level to identify several proteins that are implicated in GPVI signaling in human platelets. In our study, immunoprecipitation of tyrosine phosphorylation at the peptide level combined with stable isotope labeling-based quantitation adds much additional detail. For instance, we were able to identify the specific phosphorylation sites on the earlier implicated proteins (DOK2 [Tyr299], MAPK14 [Tyr182], and nonreceptor type protein tyrosine phosphatase 6/SHP-1 [Tyr64]), and quantified their relative upregulation on GPVI stimulation. The 3 novel platelet proteins with increased tyrosine phosphorylation downstream of GPVI seem valid novel additions to the downstream GPVI signaling cascades. ABL1 (Tyr393) and

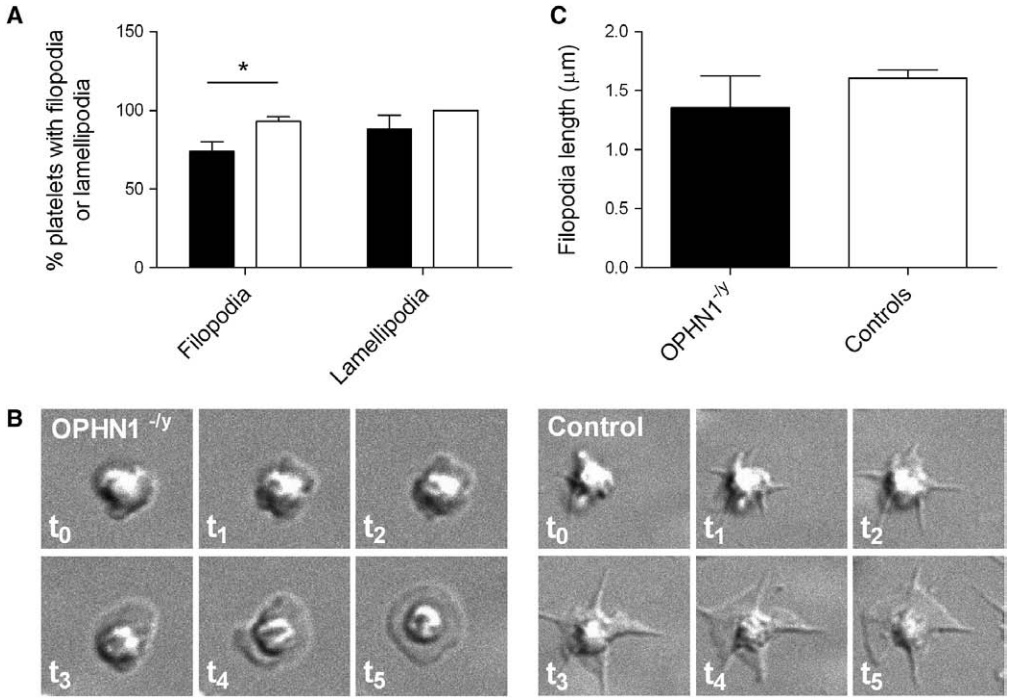

Figure 4. Filopodia formation in platelets of oligophrenin-1 (OPHN1)$^{-/y}$ patients and controls. OPHN1 deficiency is associated with decreased filopodia formation before spreading on cross-linked collagen-related peptide (CRP-XL)/GFOGER-coated coverslips. **A**, Platelet-rich plasma of 4 OPHN1$^{-/y}$ patients (black bars) and 5 healthy controls (white bars) containing RGD was perfused over CRP-XL/GFOGER-coated cover glasses at 25/s for 20 minutes. Pictures were taken every 10 seconds. Filopodia formation and subsequent lamellipodia formation were counted and expressed as a percentage of total quantified platelets. Data are shown as mean percentage±95% confidence interval. Differences between patients and controls were significant (*Wilcoxon rank $P<0.05$). **B**, Snapshots of a platelet from an OPHN1$^{-/y}$ patient (**top**) and a healthy control (**bottom**) adhering and spreading at increasing time points (t_0 to t_5, corresponding to ≈0 [adhesion], 100, 200, 300, 400, and 500 s, respectively), perfused over CRP-XL/GFOGER. **C**, Filopodia length of OPHN1$^{-/y}$ and control platelets perfused over CRP-XL/GFOGER-coated coverslips as described for **A**.

ABL2 (Tyr439; the observed tyrosine-phosphorylated peptide is present in both isoforms) regulate cytoskeletal reorganization in several myeloid cell types[23] and known ABL interactors such as Src family kinases, GADS, NCK1, and SLP-76 are also found regulated in this study. Given the importance of cytoskeletal rearrangement in platelet activation, the presence of ABL and its phosphorylation in platelets are not unexpected.

Nonreceptor type protein tyrosine phosphatase 18 is a member of the PEST family of protein tyrosine phosphatases. Little is known about its biological function, although overexpression studies suggested a role in neurite outgrowth and actin cytoskeleton reorganization.[24] Nonreceptor type protein tyrosine phosphatase 18 is regulated by tyrosine phosphorylation, including the GPVI downstream target site discovered in the present study (Tyr389).

Our attention was drawn to the potential impact of OPHN1 deficiency on platelet function. In patients with *OPHN1* mutations, loss or dysfunction of OPHN1 is associated with reduced dendritic spine and filopodia length of neurons, the molecular explanation of their neurological phenotype.[20,21] In neurons, OPHN1 localizes to filopodia, lamellipodia, and stress fibers to regulate the actin cytoskeleton.[20,25,26] To determine the platelet phenotype, here a thorough functional screen of the platelets of patients with oligophrenia was performed. On the basis of several standard functional tests, OPHN1-deficient platelets seemed hemostatically normal, with no exception for the clot retraction assay, a measure for actin cytoskeleton contractility in which we expected to see differences because of the strong effects on filopodia length in neurons. The single phenotype we found was reduced filopodia formation of platelets during spreading on a collagen-like surface, but not on fibrinogen, indicative of the specific function of OPHN1 in human platelets.

Recently, Elvers et al[27] reported a study on the presence of OPHN1 in human and murine platelets and its Rho-GTPase activity toward RhoA, Cdc42, and Rac1 in an A5-Chinese hamster ovary cell culture model system. They showed that on platelet spreading on fibrinogen, OPHN1 colocalized with actin in filopodia, the actin ring, and lamellipodia. In addition, OPHN1 colocalized with Rac1 and Cdc42 in the late phase of platelet spreading on fibrinogen, whereas RhoA colocalization was observed independent of activation and spreading. In our experiments, we could not confirm a role for OPHN1 in platelet spreading on fibrinogen. Given the data of Elvers et al,[27] OPHN1 may have a redundant role in platelet spreading on fibrinogen in human platelets, which becomes apparent when overexpressed.

On collagen, we found a more pronounced role for the Rho GTPase–activating protein because its absence leads to reduced filopodia formation before spreading. In the experiments of Elvers et al,[27] overexpression of OPHN1 in A5-Chinese hamster ovary cells inhibited lamellipodia formation. This may be consistent with the observed phenotype in this article (Figure 4) because the balance toward lamellipodia formation by absence of OPHN1 may overrule the formation of filopodia, causing platelets to spread without the formation of filopodia.

In conclusion, we identified 28 pTyr sites on 27 proteins, which undergo >2-fold increase in phosphorylation on GPVI activation in human platelets. We discovered 3 novel factors that are involved downstream of GPVI signaling after platelet activation, one of which was OPHN1. In response to GPVI stimulation, OPHN1 becomes phosphorylated at Tyr370 and plays a role in the formation of filopodia during platelet spreading on collagen.

Acknowledgments

We thank A.D. Barendrecht, C.A. Koekman, B. Rutten, Dr Angelis, and Z. Iqbal for technical assistance, and Dr Watson for critically reviewing our article.

Sources of Funding

This research was performed within the framework of the Center for Translational Molecular Medicine (www.ctmm.nl), project CIRCULATING CELLS (grant 01C-102), and was supported by The Netherlands Heart Foundation. The Netherlands Proteomics Center embedded in the Netherlands Genomics Initiative is kindly acknowledged for financial support (A.J.R. Heck, A. Scholten). The Cardiovascular Focus en Massa Programma at Utrecht University is acknowledged for additional financial support (A. Scholten).

Disclosures

None.

References

1. Wei AH, Schoenwaelder SM, Andrews RK, Jackson SP. New insights into the haemostatic function of platelets. *Br J Haematol*. 2009;147:415–430.
2. Massberg S, Gawaz M, Grüner S, Schulte V, Konrad I, Zohlnhöfer D, Heinzmann U, Nieswandt B. A crucial role of glycoprotein VI for platelet recruitment to the injured arterial wall in vivo. *J Exp Med*. 2003;197:41–49.
3. Nieswandt B, Watson SP. Platelet-collagen interaction: is GPVI the central receptor? *Blood*. 2003;102:449–461.
4. Auger JM, Kuijpers MJ, Senis YA, Watson SP, Heemskerk JW. Adhesion of human and mouse platelets to collagen under shear: a unifying model. *FASEB J*. 2005;19:825–827.
5. Stoll G, Kleinschnitz C, Nieswandt B. Molecular mechanisms of thrombus formation in ischemic stroke: novel insights and targets for treatment. *Blood*. 2008;112:3555–3562.
6. Takayama H, Hosaka Y, Nakayama K, Shirakawa K, Naitoh K, Matsusue T, Shinozaki M, Honda M, Yatagai Y, Kawahara T, Hirose J, Yokoyama T, Kurihara M, Furusako S. A novel antiplatelet antibody therapy that induces cAMP-dependent endocytosis of the GPVI/Fc receptor gamma-chain complex. *J Clin Invest*. 2008;118:1785–1795.
7. Boylan B, Berndt MC, Kahn ML, Newman PJ. Activation-independent, antibody-mediated removal of GPVI from circulating human platelets: development of a novel NOD/SCID mouse model to evaluate the *in vivo* effectiveness of anti-human platelet agents. *Blood*. 2006;108:908–914.
8. Barrow AD, Trowsdale J. You say ITAM and I say ITIM, let's call the whole thing off: the ambiguity of immunoreceptor signalling. *Eur J Immunol*. 2006;36:1646–1653.
9. Watson SP, Auger JM, McCarty OJ, Pearce AC. GPVI and integrin alphaIIb beta3 signaling in platelets. *J Thromb Haemost*. 2005;3:1752–1762.
10. Watson SP, Herbert JM, Pollitt AY. GPVI and CLEC-2 in hemostasis and vascular integrity. *J Thromb Haemost*. 2010;8:1456–1467.
11. Boersema PJ, Foong LY, Ding VM, Lemeer S, van Breukelen B, Philp R, Boekhorst J, Snel B, den Hertog J, Choo AB, Heck AJ. In-depth qualitative and quantitative profiling of tyrosine phosphorylation using a combination of phosphopeptide immunoaffinity purification and stable isotope dimethyl labeling. *Mol Cell Proteomics*. 2010;9:84–99.
12. Rikova K, Guo A, Zeng Q, et al. Global survey of phosphotyrosine signaling identifies oncogenic kinases in lung cancer. *Cell*. 2007;131:1190–1203.
13. Zhang Y, Wolf-Yadlin A, Ross PL, Pappin DJ, Rush J, Lauffenburger DA, White FM. Time-resolved mass spectrometry of tyrosine phosphorylation sites in the epidermal growth factor receptor signaling network reveals dynamic modules. *Mol Cell Proteomics*. 2005;4:1240–1250.
14. Farndale RW, Lisman T, Bihan D, Hamaia S, Smerling CS, Pugh N, Konitsiotis A, Leitinger B, de Groot PG, Jarvis GE, Raynal N. Cell-collagen interactions: the use of peptide Toolkits to investigate collagen-receptor interactions. *Biochem Soc Trans*. 2008;36(pt 2):241–250.
15. Ding VM, Boersema PJ, Foong LY, Preisinger C, Koh G, Natarajan S, Lee DY, Boekhorst J, Snel B, Lemeer S, Heck AJ, Choo A. Tyrosine phosphorylation profiling in FGF-2 stimulated human embryonic stem cells. *PLoS One*. 2011;6:e17538.
16. García A, Senis YA, Antrobus R, Hughes CE, Dwek RA, Watson SP, Zitzmann N. A global proteomics approach identifies novel phosphorylated signaling proteins in GPVI-activated platelets: involvement of G6f, a novel platelet Grb2-binding membrane adapter. *Proteomics*. 2006;6:5332–5343.
17. Senis YA, Antrobus R, Severin S, Parguiña AF, Rosa I, Zitzmann N, Watson SP, García A. Proteomic analysis of integrin alphaIIbbeta3 outside-in signaling reveals Src-kinase-independent phosphorylation of Dok-1 and Dok-3 leading to SHIP-1 interactions. *J Thromb Haemost*. 2009;7:1718–1726.
18. Zahedi RP, Lewandrowski U, Wiesner J, Wortelkamp S, Moebius J, Schütz C, Walter U, Gambaryan S, Sickmann A. Phosphoproteome of resting human platelets. *J Proteome Res*. 2008;7:526–534.
19. Billuart P, Bienvenu T, Ronce N, et al. Oligophrenin-1 encodes a rhoGAP protein involved in X-linked mental retardation. *Nature*. 1998;392:923–926.
20. Govek EE, Newey SE, Akerman CJ, Cross JR, Van der Veken L, Van Aelst L. The X-linked mental retardation protein oligophrenin-1 is required for dendritic spine morphogenesis. *Nat Neurosci*. 2004;7:364–372.
21. Nadif Kasri N, Nakano-Kobayashi A, Malinow R, Li B, Van Aelst L. The Rho-linked mental retardation protein oligophrenin-1 controls synapse maturation and plasticity by stabilizing AMPA receptors. *Genes Dev*. 2009;23:1289–1302.
22. Inoue O, Suzuki-Inoue K, Dean WL, Frampton J, Watson SP. Integrin alpha2beta1 mediates outside-in regulation of platelet spreading on collagen through activation of Src kinases and PLCgamma2. *J Cell Biol*. 2003;160:769–780.
23. Gu JJ, Ryu JR, Pendergast AM. Abl tyrosine kinases in T-cell signaling. *Immunol Rev*. 2009;228:170–183.
24. Veillette A, Rhee I, Souza CM, Davidson D. PEST family phosphatases in immunity, autoimmunity, and autoinflammatory disorders. *Immunol Rev*. 2009;228:312–324.
25. Fauchereau F, Herbrand U, Chafey P, Eberth A, Koulakoff A, Vinet MC, Ahmadian MR, Chelly J, Billuart P. The RhoGAP activity of OPHN1, a new F-actin-binding protein, is negatively controlled by its amino-terminal domain. *Mol Cell Neurosci*. 2003;23:574–586.
26. Khelfaoui M, Denis C, van Galen E, de Bock F, Schmitt A, Houbron C, Morice E, Giros B, Ramakers G, Fagni L, Chelly J, Nosten-Bertrand M, Billuart P. Loss of X-linked mental retardation gene oligophrenin1 in mice impairs spatial memory and leads to ventricular enlargement and dendritic spine immaturity. *J Neurosci*. 2007;27:9439–9450.
27. Elvers M, Beck S, Fotinos A, Ziegler M, Gawaz M. The GRAF family member oligophrenin1 is a RhoGAP with BAR domain and regulates Rho GTPases in platelets. *Cardiovasc Res*. 2012;94:526–536.

Significance

Central to their hemostatic function, platelets are capable of rapidly adhering to exposed subendothelial collagen. The immunoglobulin glycoprotein (GP) VI is the major receptor mediating platelet activation by collagen, and the GPVI signaling pathway is considered a promising target for novel antiplatelet therapies. As site-specific knowledge of phosphorylation-based signaling downstream of GPVI is still limited, it is important to improve our molecular knowledge of GPVI signaling. In a quantitative phosphoproteomics approach using immunoprecipitation of tyrosine-phosphorylated peptides and mass spectrometry, we quantitatively assessed the specific tyrosine residues that become increasingly phosphorylated at the onset of human platelet activation through GPVI. Among an interesting set of novel players, oligophrenin-1 was identified as a novel signaling protein downstream of GPVI in human platelets. Functional characterization of platelets deficient in oligophrenin-1, in essence a human knockout, implicates a role for this protein in filopodia formation on collagen, an important parameter of platelet hemostatic function.

Supplemental Data

Supplementary to: "Targeted Phosphotyrosine Profiling of GPVI Signaling Implicates Oligophrenin-1 in Platelet Filopodia Formation" by Bleijerveld *et al.* (2013*)*

Supplementary Figure I - Correlation between 5 minutes CRP-XL and 30 minutes CRP-XL experiment

Platelets were kept in a resting state (Ctrl) or stimulated with CRP-XL for 5 or 30 minutes. (A) Using MSQuant software, the ratio [Heavy/Light] = [CRP-XL/Ctrl] was calculated for immunoprecipitatedphosphotyrosine (pY)-containing peptides (red dots) and normalized on the ratio of non-phosphorylated peptides (blue dots), based on the extracted ion chromatograms of the differentially labeled isotopomers of each peptide. Peptide ratios (2Log values) were plotted against peptide abundance (intensity, 10Log values). (B) Histogram representation of panel A. Peptides were binned into [CRP-XL/Ctrl] ratio categories and the number of peptides was plotted against the [CRP-XL/Ctrl] ratio. Whereas all non-phosphorylated peptides (blue histogram) exhibit a heavy/light ratio between -1 and +1 (2Log), the pY peptide population (red histogram) clearly contains up-regulated peptides in GPVI-activated platelets. For both time points, pY peptides were considered significantly up-regulated when [CRP-XL/resting] ≥ 2-fold (2Log value of 1). (C) The [CRP-XL/Ctrl] ratio of the 30 minutes CRP-XL experiment was plotted against the [CRP-XL/Ctrl] ratio of the 5 minutes CRP-XL experiment (2LOG scale in both cases) for all pY peptides that were quantified in both experiments. Green dots represent peptides with significantly up- or down-regulated pY sites (i.e. 2Log([CRP-XL/Ctrl]) ≤ -1 or 2Log([CRP-XL/Ctrl] ≥ 1, threshold is indicated with dashed circle).

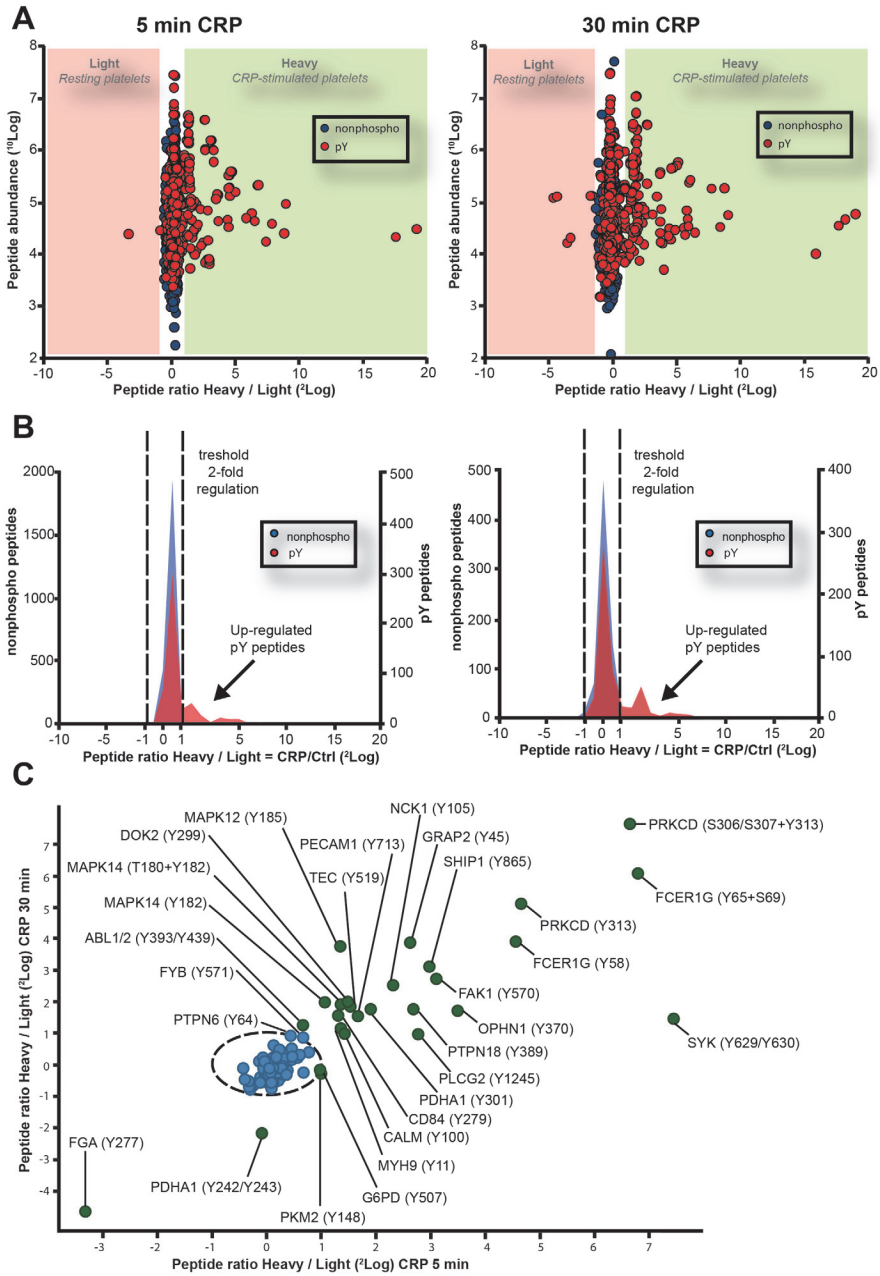
A
5 min CRP
30 min CRP
Light
Resting platelets
Heavy
CRP-stimulated platelets
nonphospho
pY
Peptide abundance (10Log)
Peptide ratio Heavy / Light (2Log)
B
treshold
2-fold
regulation
Up-regulated
pY peptides
nonphospho peptides
pY peptides
Peptide ratio Heavy / Light = CRP/Ctrl (2Log)
C
MAPK12 (Y185)
DOK2 (Y299)
MAPK14 (T180+Y182)
MAPK14 (Y182)
ABL1/2 (Y393/Y439)
FYB (Y571)
PTPN6 (Y64)
FGA (Y277)
PDHA1 (Y242/Y243)
PKM2 (Y148)
G6PD (Y507)
MYH9 (Y11)
CALM (Y100)
CD84 (Y279)
PDHA1 (Y301)
PLCG2 (Y1245)
PTPN18 (Y389)
OPHN1 (Y370)
FAK1 (Y570)
SHIP1 (Y865)
GRAP2 (Y45)
NCK1 (Y105)
PECAM1 (Y713)
TEC (Y519)
PRKCD (S306/S307+Y313)
FCER1G (Y65+S69)
PRKCD (Y313)
FCER1G (Y58)
SYK (Y629/Y630)
Peptide ratio Heavy / Light (2Log) CRP 30 min
Peptide ratio Heavy / Light (2Log) CRP 5 min

Supplementary Figure II - GPVI response proteome

Proteins involved in GPVI signaling (adapted from Watson *et al.* [1]). Crosslinking of GPVI by collagen or CRP-XL induces tyrosine phosphorylation of the FcRγ-chain ITAM by the Src family kinases, Fyn and Lyn, which are constitutively bound to the proline-rich region in the GPVI cytosolic tail. This initiates a Syk-dependent signaling cascade that leads to the formation of a LAT signalosome and activation of PLCγ2. PLCγ2 associates directly with LAT, and indirectly via the adapters Gads and SLP-76. PLCγ2 also associates with the membrane via binding of its PH domain to PIP3. Functional homologues from the Tec and Vav families support activation of PLCγ2.

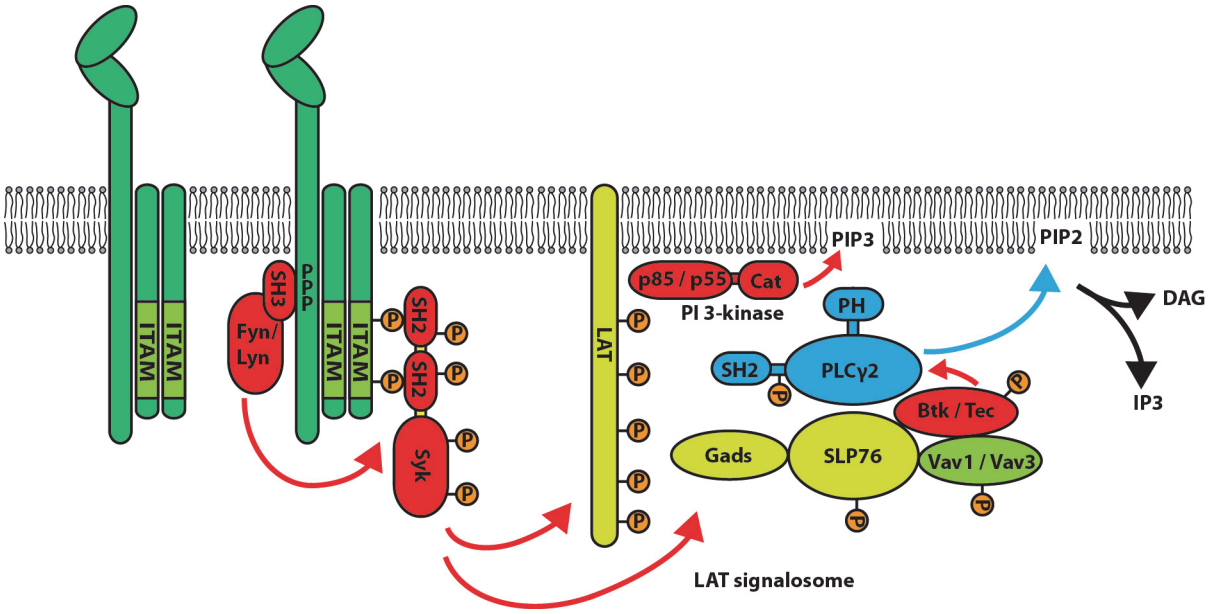

Supplementary Figure III - Oligophrenin-1 deficient platelets respond normal to activation.

Oligophrenin-1 deficiency of four OPHN1$^{-/y}$ patients (black traingles) is not associated with significantly increased (A) P-selectin expression and (B) $\alpha_{IIb}\beta3$ activation compared to nine controls (white blocks). Platelets were stimulated with increasing concentrations of ADP, TRAP, and CRP-XL. Expression of P-selectin and $\alpha_{IIb}\beta3$ activation was determined by FACS analysis with mouse-anti P-selectin-PE, and fibrinogen-FITC respectively. The mean of the percentage of P-selectin expression, and $\alpha_{IIb}\beta3$ activation with ± SD is shown. Differences between patients and controls for each concentration of agonists were non-significant (Wilcoxon's rank $P > 0.05$).

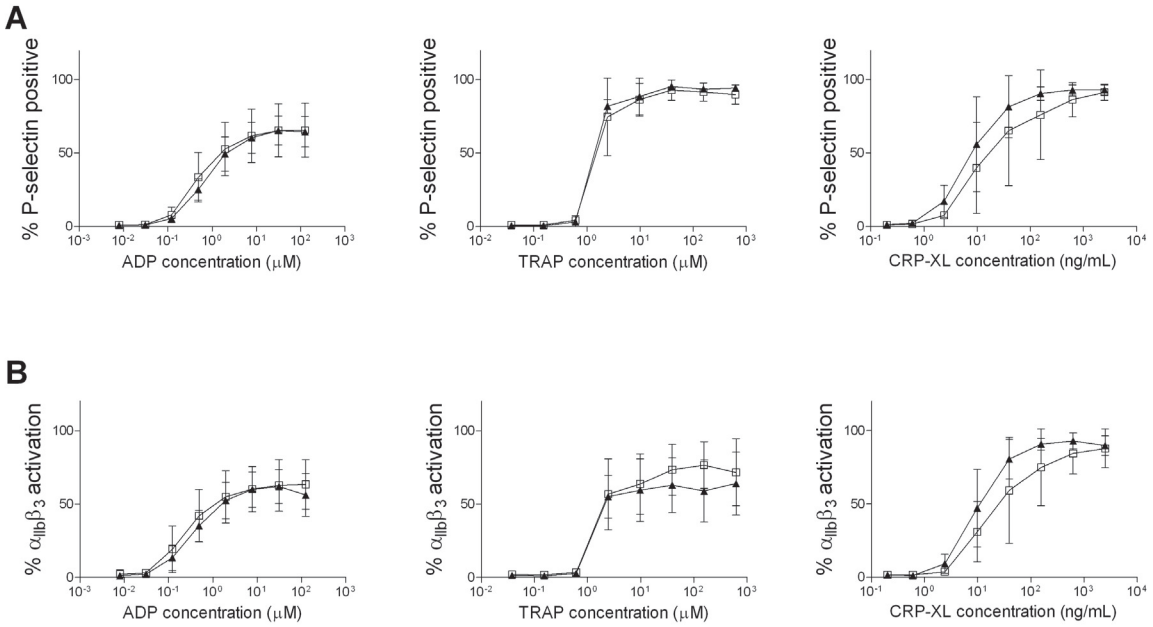

Supplementary Figure IV - Oligophrenin-1 deficient platelets form normal aggregates
(A) Whole blood of an OPHN1$^{-/y}$ patient and three healthy controls was perfused over collagen coated coverslips. Pictures were taken every 10 seconds. Representative pictures are shown. (B) Surface coverage of platelets from an OPHN1$^{-/y}$ patient (black triangles) and three healthy controls (white squares) on collagen coated cover glasses was determined at the indicated time points by pixel count using Image J. Perfusions were performed in duplicate of which the mean was calculated. Data are expressed as mean ± 95% confidence interval of the mean of duplicate experiments.

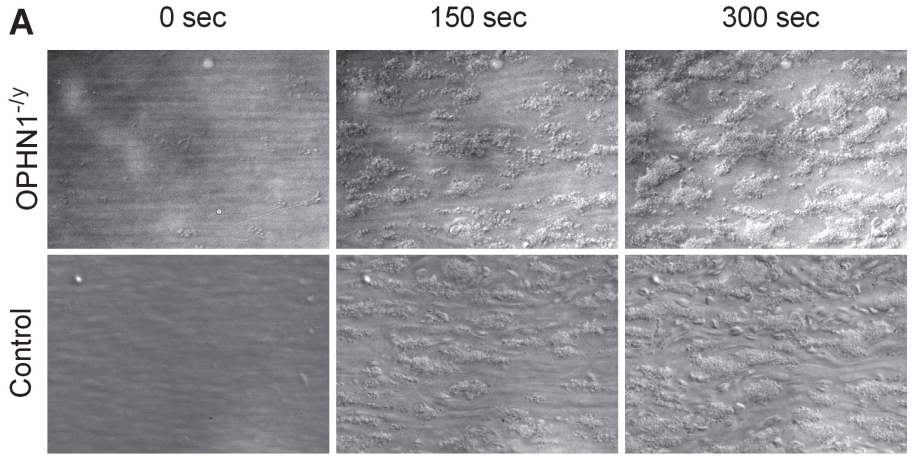

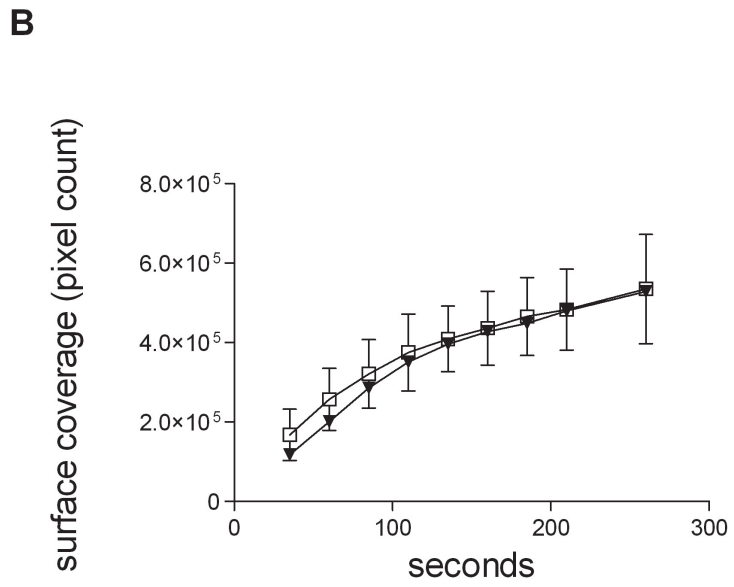

Supplementary Figure V - Oligophrenin-1 deficiency is not associated with altered clot retraction compared to healthy controls

(A) PRP of a single OPHN1$^{-/y}$ patient was stimulated with a PAR-1 peptide. Pictures were taken at indicated time points. (B) Clot size of an OPHN1$^{-/y}$ patient (black triangles) and three healthy controls (white squares) was determined by pixel count using Image J. Experiments were performed in quadruplicate and the mean was taken. Data are represented as mean ± 95% confidence interval of the mean of quadruplicate measurements of three healthy controls.

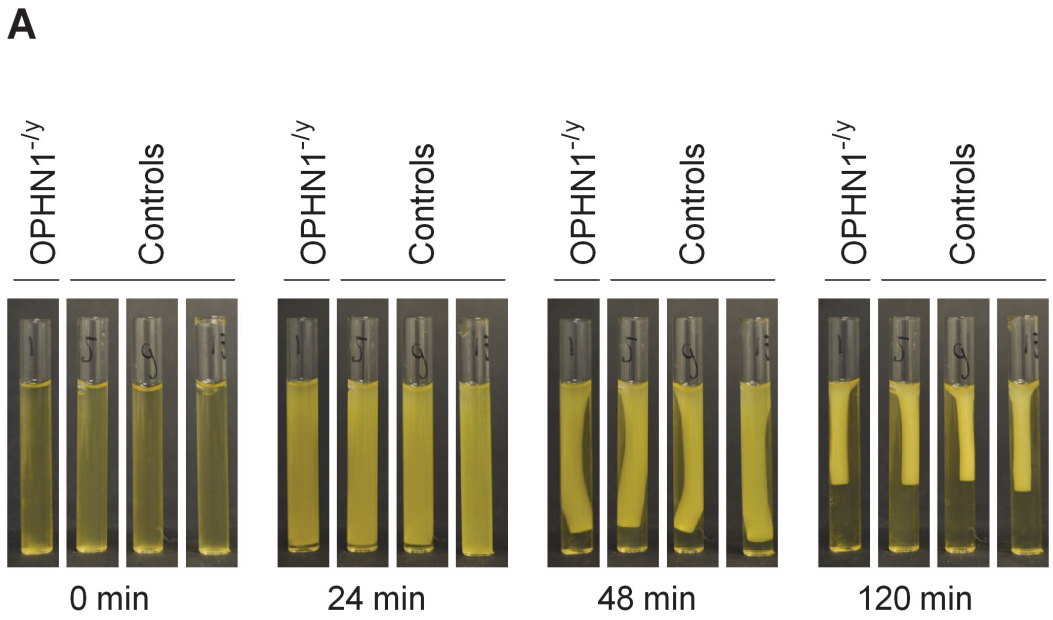

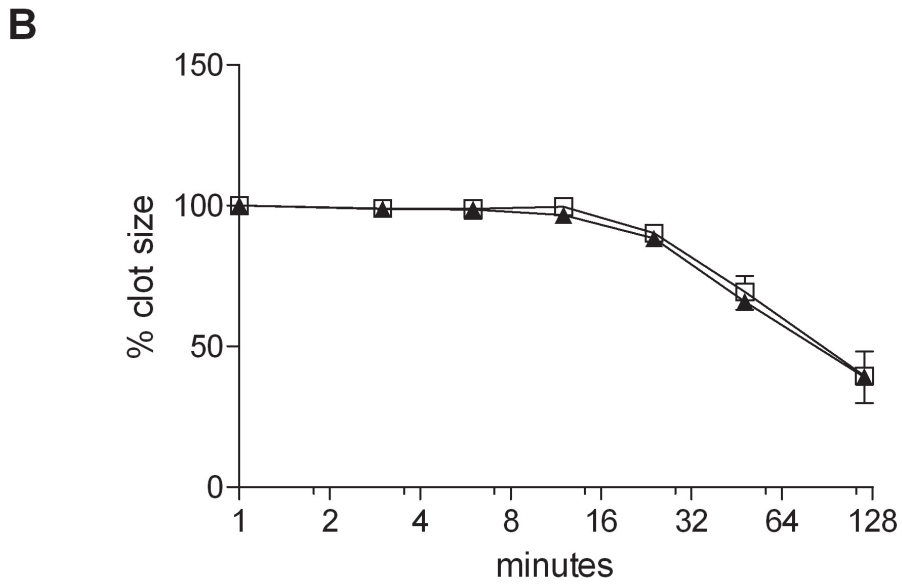

Supplementary Video 1.

Spreading of an oligophrenin-1 deficient platelet on CRP-XL/GFOGER in presence of 0.5 mM RGD.

Supplementary Video 2.

Spreading of a healthy donor platelet on CRP-XL/GFOGER in presence of 0.5 mM RGD.

References

1. Watson SP, Auger JM, McCarty OJ, Pearce AC. Gpvi and integrin alphaiib beta3 signaling in platelets. *Journal of thrombosis and haemostasis : JTH*. 2005;3:1752-1762

Supplementary Table I - Phosphotyrosine peptides identified and quantified after CRP treatment. Supplemental to Bleijerveld *et al.* 2012

List of all phosphotyrosine peptides identified (manually scrutinized) and quantified after CRP treatment. pY, phosphotyrosine; pT, phosphothreonine; pS, phosphoserine.

In some cases, MS/MS fragments were not sufficient for site localization, these are indicated with /

=Peptide with increased tyrosine phosphorylation upon CRP-XL treatment

Swissprot Accession Number	Gene	Protein name	Phosphotyrosine peptide	Phosphosite	Ratio (CRP/Ctrl) 5 min	Ratio (CRP/Ctrl) 30 min
P21333	FLNA	Filamin-A	VANPSGNLTETpYVQDR	Y1308	1.2	0.9
			VHSPSGALEECpYVTEIDQDK	Y2379	1.1	1.2
			SPFEVpYVDK	Y373		0.9
Q9Y490	TLN1	Talin-1	ALDpYYMLR	Y70/Y71	1.1	0.9
			TMQFEPSTMVpYDACR	Y26	1.0	0.8
			AGALQCSPSDApYTK	Y1945		1.3
			EAApYHPEVAPDVR	Y2224		1.0
			IGITNHDEpYSLVR	Y127		0.9
P35579	MYH9	Myosin-9	ALELDSNLpYR	Y754	1.1	0.9
			VIQpYLAYVASSHK	Y190	1.3	1.0
			VIQYLApYVASSHK	Y193	1.2	
			YLpYVDK	Y11	2.6	2.2
P60709	ACTB	Actin, cytoplasmic 1	DLTDpYLMK	Y188	1.1	1.0
			DSpYVGDEAQSK	Y53	1.3	1.4
			GpYSFTTTAER	Y198	1.4	1.1
			QEpYDESGPSIVHR	Y362	1.5	1.2
			IWHHTFpYNELR	Y91		0.9
P07996	THBS1	Thrombospondin-1	AQGpYSGLSVK	Y1058	1.1	0.7
			DNCPNLPNSGQEDpYDK	Y729	1.1	0.7
			IMADSGPIpYDK	Y1139	1.0	0.7
			CTSpYPDGSWK	Y565		0.6
			DNCQpYVYNVDQR	Y815		0.9
			DNCQYVpYNVDQR	Y817	1.0	0.8
			RPPLCpYHNGVQYR	Y319		0.7
			VVMpYEGKK	Y1126		0.5
P18206	VCL	Vinculin	SFLDSGpYR	Y822	1.1	1.5
P02671	FGA	Fibrinogen alpha chain	GGSTSpYGTGSETESPR	Y277	0.1	0.0
			QFTSSTSpYNR	Y589		0.6
P05106	ITGB3	Integrin beta-3	EATSTFTNITpYR	Y785	1.1	0.9
			FQpYYEDSSGK	Y695	1.1	1.0
			WDTANNPLpYK	Y773	1.1	1.0
P49840	GSK3A	Glycogen synthase kinase-3 alpha	GEPNVSpYICSR	Y279	1.2	0.9
P23528	CFL1	Cofilin-1	HELQANCpYEEVK	Y140	1.0	0.8
			YALYDATpYETK	Y89	1.1	0.7
P07737	PFN1	Profilin-1	CpYEMASHLR	Y129	1.1	0.8
P14618	PKM2	Pyruvate kinase isozymes M1/M2	ITLDNApYMEK	Y148	2.0	0.8
P06241	FYN	Tyrosine-protein kinase Fyn	GApYSLSIR	Y185	1.1	0.9
			LDNGGpYITTR	Y213	1.1	0.9
			LIEDNEpYTAR	Y420	0.9	1.1
			WTAPEAALpYGR	Y440	1.0	1.0
P07948	LYN	Tyrosine-protein kinase Lyn	SLDNGGYpYISPR	Y194	1.0	0.8
			VENCPDELpYDIMK	Y473	0.9	0.8
			VIEDNEpYTAR	Y397	0.7	0.9
Q16539	MAPK14	Mitogen-activated protein kinase 14 (p38 alpha)	HTDDEMTGpYVATR	Y182	2.6	3.8
			HTDDEMpTGpYVATR	T180+Y182	2.1	4.0
P50552	VASP	Vasodilator-stimulated phosphoprotein	ATVMLpYDDGNK	Y16	1.2	0.8
			VQIpYHNPTANSFR	Y39	1.1	0.8
Q86UX7	FERMT3	Fermitin family homolog 3	EKEPEEELpYDLSK	Y162	1.1	1.0
			TASGDpYIDSSWELR	Y11	1.0	1.1
			ETTLSpYYK	Y387/Y388	2.0	
P11142	HSPA8	Heat shock cognate 71 kDa protein	TTPSpYVAFTDTER	Y41	0.8	0.6
			VQVEpYK	Y107	1.4	
P08238	HSP90AB1	Heat shock protein HSP 90-beta	SIpYYITGESK	Y484	1.2	0.8
P62158	CALM1	Calmodulin	DGNGpYISAAELR	Y100	2.7	2.0
Q04837	SSBP1	Single-stranded DNA-binding protein, mitochondrial	SGDSEVpYQLGDVSQK	Y73	1.2	1.0
Q01518	CAP1	Adenylyl cyclase-associated protein 1	QVAYIpYK	Y354	1.1	0.9
			EMNDAAMFpYTNR	Y164		0.8
Q06124	PTPN11	Tyrosine-protein phosphatase non-receptor type 11 (SHP-2)	IQNTGDpYYDLYGGEK	Y62	1.2	0.9
			IQNTGDYYDLpYGGEK	Y66		1.5
P30273	FCER1G	High affinity immunoglobulin epsilon receptor subunit gamma (FcR gamma)	AAITSpYEK	Y58	23.5	15.0
			SDGVpYTGLpSTR	Y65+S69	110.5	67.2
P02775	PPBP	Platelet basic protein	GKEESLDSDLpYAELR	Y58	0.5	
P21291	CSRP1	Cysteine and glycine-rich protein 1	CSQAVpYAAEK	Y127	1.1	0.9
Q05655	PRKCD	Protein kinase C delta type	GRGEpYFAIK	Y374	1.1	0.9
			SDSASSEPVGIpYQGFEK	Y313	88.7	34.5
			SDpSASSEPVGIpYQGFEK	S304/S306/S307 + Y313	>100	>200
			STFDAHIYEGR	Y64	1.2	0.8
Q9HBI1	PARVB	Beta-parvin	QLEEDLpYDGQVLQK	Y116	1.2	0.8
P12931	SRC	Proto-oncogene tyrosine-protein kinase Src	GApYCLSVSDFDNAK	Y187	1.2	0.9
			LDSGGFpYITSR	Y216	1.1	0.9
			LIEDNEpYTAR	Y419		1.1
			WTAPEAALpYGR	Y439		1.0
Q86Z02	HIPK1	Homeodomain-interacting protein kinase 1	AVCSTpYLQSR	Y352	1.2	0.8
			AVCSTpYLQpSR	Y352+S355	1.1	0.9
Q13201	MMRN1	Multimerin-1	MTDQVNpYQAMK	Y330	1.1	0.9
P30041	PRDX6	Peroxiredoxin-6	DINApYNCEEPTEK	Y89	1.0	0.8
O75563	SKAP2	Src kinase-associated phosphoprotein 2	RIpYQFTAASPK	Y197	1.1	0.8
			TVFYpYYGSDK	Y151	1.2	0.9
			pYGWWVGEMK	Y331	1.2	1.0
P42680	TEC	Tyrosine-protein kinase Tec	YVLDDQpYTSSSGAK	Y519	2.9	3.6
P08567	PLEK	Pleckstrin	EGpYLVK	Y10	1.6	0.9
Q13627	DYRK1A	Dual specificity tyrosine-phosphorylation-regulated kinase 1A	IYQpYIQSR	Y321	1.2	0.9
P07195	LDHB	L-lactate dehydrogenase B chain	MVVESApYEVIK	Y240	1.1	0.9
P51659	HSD17B4	Peroxisomal multifunctional enzyme type 2	AVANpYDSVEEGEK	Y73	1.3	1.0
O00116	AGPS	Alkyldihydroxyacetonephosphate synthase, peroxisomal	QVpYDIAAK	Y485	1.2	0.9
			IRPVPEpYQK	Y387	1.0	
			ETNISpYSQEADDR	Y175		0.8
			WNGWGpYNDSK	Y98		1.0
P06239	LCK	Tyrosine-protein kinase Lck	NLDNGGFpYISPR	Y192	1.2	1.1
P50851	LRBA	Lipopolysaccharide-responsive and beige-like anchor protein	SIVEEEEDDDpYVELK	Y1110	0.8	0.6
O15117	FYB	FYN-binding protein	TTAVEIDpYDSLK	Y571	1.6	1.9
			VLpYSTK	Y709	2.8	
P00338	LDHA	L-lactate dehydrogenase A chain	QVVESApYEVIK	Y239	1.1	0.9
Q9H422	HIPK3	Homeodomain-interacting protein kinase 3	TVCSTpYLQSR	Y359	1.1	0.8
P08559	PDHA1	Pyruvate dehydrogenase E1 component subunit alpha, somatic form, mitochon	AAASTDpYYK	Y242	0.9	0.2
			AAASTDYpYK	Y243	0.8	0.1
			pYHGHSMSDPGVSYR	Y289		1.4
			YHGHSMSDPGVSpYR	Y301	3.7	3.4
			YHGHpSMSDPGVSpYR	S293+Y301	1.7	1.3
P16284	PECAM1	Platelet endothelial cell adhesion molecule	DTETVpYSEVR	Y713	3.2	2.9
Q99952	PTPN18	Tyrosine-protein phosphatase non-receptor type 18	SAEEAPLpYSK	Y389	6.4	3.4
Q9UBW5	BIN2	Bridging integrator 2	LNHNLpYEVMSK	Y232	1.3	0.9
			DVFpYR	Y221	1.1	
Q9NRY4	GRLF1	Glucocorticoid receptor DNA-binding factor 1	NEEENIpYSVPHDSTQGK	Y1105	1.4	1.4
Q05397	FAK1	Focal adhesion kinase 1	pYMEDSTYYK	Y570	8.6	6.6

P26599	PTBP1	Polypyrimidine tract-binding protein 1	GQPIpYIQFSNHK	Y127	1.2	1.0
Q9Y316	MEMO1	Protein MEMO1	YSYYDESQGEIpYR	Y210	1.1	0.9
P53990	KIAA0174	IST1 homolog	EIADpYLAAGK	Y43	1.0	0.8
P45983	MAPK8	Mitogen-activated protein kinase 8 (c-Jun terminal kinase JNK1)	TAGTSFMMTPpYVVTR	Y185	1.2	1.1
P16333	NCK1	Cytoplasmic protein NCK1	ETVpYCIGQR	Y339	1.0	1.0
			LpYDLNMPAYVK	Y105	4.9	5.8
O43639	NCK2	Cytoplasmic protein NCK2	VQLVDNVpYCIGQR	Y342	1.0	1.0
P00519/P42684	ABL1/ABL2	Tyrosine-protein kinase ABL1 / ABL2	LMTGDTpYTAHAGAK	Y393(ABL1)/Y439 (ABL2)	1.6	2.4
Q00610	CLTC	Clathrin heavy chain 1	ENPpYYDSR	Y899	1.2	1.2
P29350	PTPN6	Tyrosine-protein phosphatase non-receptor type 6 (SHP-1)	EDVpYENLHTK	Y564	1.2	1.4
			IQNSGDFYDLpYGGEK	Y64	1.4	1.9
			QPYpYATR	Y214		0.8
P37840	SNCA	Alpha-synuclein	EGVLpYVGSK	Y39	1.2	0.8
O60496	DOK2	Docking protein 2	GQEGEpYAVPFDAVAR	Y299	2.8	4.0
P45984	MAPK9	Mitogen-activated protein kinase 9 (c-Jun terminal kinase JNK2)	TACTNFMMTPpYVVTR	Y185	1.0	1.1
P11413	G6PD	Glucose-6-phosphate 1-dehydrogenase	VGFQYEGTpYK	Y507	2.0	0.9
			VGFQpYEGTYK	Y503	1.3	
			VQPNEAVpYTK	Y401	1.1	0.9
			IDHpYLGK	Y202	1.2	0.7
P11279	LAMP1	Lysosome-associated membrane glycoprotein 1	ALQATVGNSpYK	Y336	1.2	0.9
O00459	PIK3R2	Phosphatidylinositol 3-kinase regulatory subunit beta	EYDQLpYEEYTR	Y464	1.2	0.8
Q15118	PDK1	[Pyruvate dehydrogenase [lipoamide]] kinase isozyme 1, mitochondrial	GVPGQVDFpYAR	Y49	1.2	1.0
P53778	MAPK12	Mitogen-activated protein kinase 12 (p38 gamma)	QADSEMTGpYVVTR	Y185	2.5	13.5
			QADSEMpTGpYVVTR	T183+Y185		16.6
O75791	GRAP2	GRB2-related adapter protein 2 (GADS)	AELGSQEGpYVPK	Y45	6.2	14.6
P29597	TYK2	Non-receptor tyrosine-protein kinase TYK2	LLAQAEGEPCpYIR	Y292	0.8	0.6
P05556	ITGB1	Integrin beta-1	WDTGENPIpYK	Y783	1.0	1.2
P53396	ACLY	ATP-citrate synthase	TTDGVpYEGVAIGGDR	Y682	1.1	0.8
P42229	STAT5A	Signal transducer and activator of transcription 5A	AVDGpYVKPQIK	Y694	1.5	1.2
			LGHpYATQLQK	Y90		0.7
P00558	PGK1	Phosphoglycerate kinase 1	ELNpYFAK	Y196	1.2	
Q7L7X3	TAOK1	Serine/threonine-protein kinase TAO1	ELDNLQpYR	Y309	1.1	0.7
Q99798	ACO2	Aconitate hydratase, mitochondrial	FNPETDpYLTGTDGK	Y513	1.1	0.9
O60890	OPHN1	Oligophrenin-1	EPIpYHSPITK	Y370	11.2	3.3
Q99613	EIF3C	Eukaryotic translation initiation factor 3 subunit C	QGTpYGGYFR	Y881	1.0	0.9
P61006	RAB8A	Ras-related protein Rab-8A	TpYDYLFK or TYDpYLFK	Y5/Y7	1.1	1.0
Q9NP81	SARS2	Seryl-tRNA synthetase, mitochondrial	EGpYSALPQLDIER	Y52	1.1	0.8
P11216	PYGB	Glycogen phosphorylase, brain form	DFpYELEPEK	Y473	1.2	0.9
P25787	PSMA2	Proteasome subunit alpha type-2	SILpYDER	Y57	1.1	0.8
			HIGLVpYSGMGPDYR	Y76		0.6
Q14197	ICT1	Immature colon carcinoma transcript 1 protein	LpYPESQGSDTAWR	Y49	1.1	0.9
O75063	FAM20B	Protein FAM20B	DHVVEGEPpYAGYDR	Y138	1.0	0.8
Q14247	CTTN	Src substrate cortactin	LPpSSPVpYEDAASFK	S417/S418 + Y421	0.8	0.7
			SAVGFDpYQGK	Y178	1.0	0.7
Q9UIB8	CD84	SLAM family member 5	TIpYTYIMASR	Y279	2.5	3.0
P22694	PRKACB	cAMP-dependent protein kinase catalytic subunit beta	ATEQpYYAMK	Y69	1.2	0.9
Q9Y624	F11R	Junctional adhesion molecule A	VIpYSQPSAR	Y280	1.0	1.1
P16885	PLCG2	1-phosphatidylinositol-4,5-bisphosphate phosphodiesterase gamma-2	EFSVNENQLQLpYQEK	Y1245	6.8	2.0
Q7KZF4	SND1	Staphylococcal nuclease domain-containing protein 1	EpYGMIYLGK	Y109	0.9	0.7
P37802	TAGLN2	Transgelin-2	GPApYGLSR	Y8		0.8
P04075	ALDOA	Fructose-bisphosphate aldolase A	CQpYVTEK	Y204		0.8
P06733	ENO1	Alpha-enolase	AAVPSGASTGIpYEALELR	Y44		0.9
P50395	GDI2	Rab GDP dissociation inhibitor beta	TDDYLDQPCpYETINR	Y203	1.0	0.7
O43665	RGS10	Regulator of G-protein signaling 10	EIpYMTFLSSK	Y86	1.0	0.9
Q9NUM4	TMEM106B	Transmembrane protein 106B	EDApYDGVTSENMR	Y58		1.2
Q06187	BTK	Tyrosine-protein kinase BTK	HYVVCSTPQSQpYYLAEK	Y344/Y345		1.1
			YVLDDEpYTSSVGSK	Y551		2.1
Q7LDG7	RASGRP2	RAS guanyl-releasing protein 2	ALILGIpYK	Y523	0.8	0.7
Q9BSJ8	ESYT1	Extended synaptotagmin-1	HLSPpYATLTVGDSSHK	Y822	1.2	0.9
O15144	ARPC2	Actin-related protein 2/3 complex subunit 2	DDETMpYVESK	Y153		1.4
Q6VY07	PACS1	Phosphofurin acidic cluster sorting protein 1	IpYSLSSQPIDHEGIK	Y251		0.8
O60268	KIAA0513	Uncharacterized protein KIAA0513	AVTApYSPEDEK	Y278		0.8
Q5VY43	PEAR1	Platelet endothelial aggregation receptor 1	DSGTpYEQPSPLIHDR	Y979		0.8
P43405	SYK	Tyrosine-protein kinase SYK	ELNGTpYAIAGGR	Y74		1.0
			LRNpYYYDVVN	Y629/Y630	173.8	2.8
Q16644	MAPKAPK3	MAP kinase-activated protein kinase 3	LLpYDSPK	Y76		1.0
P63167	DYNLL1	Dynein light chain 1, cytoplasmic	NFGSpYVTHETK	Y65		0.9
P15498	VAV1	Proto-oncogene vav	ARpYDFCAR	Y791		64.2
			GEIpYGR	Y826	1.0	
Q9NXR7	BRE	BRCA1-A complex subunit BRE	VQpYVIQGYHK	Y263		0.9
Q9Y4D1	DAAM1	Disheveled-associated activator of morphogenesis 1	AVETELEpYQK	Y912		0.8
Q92569	PIK3R3	Phosphatidylinositol 3-kinase regulatory subunit gamma	EYDRLpYEEYTR	Y199		0.9
P14625	HSP90B1	Endoplasmin	GLFDEpYGSK	Y401		1.0
P06493	CDK1	Cell division control protein 2 homolog	IGEGTYGVVpYK	Y19	1.2	0.9
Q92835	SHIP1	Phosphatidylinositol-3,4,5-trisphosphate 5-phosphatase 1	LpYDFVK	Y865	7.9	8.7
Q8N392	ARHGAP18	Rho GTPase-activating protein 18	CLDDDTpYMK	Y643	1.0	0.8
Q5JSL3	DOCK11	Dedicator of cytokinesis protein 11	TQIpYSDPLR	Y57	1.0	
O60674	JAK2	Tyrosine-protein kinase JAK2	IQDpYHILTR	Y221	1.1	0.6
			EVGDpYGQLHETEVLLK	Y570		0.7
P48147	PREP	Prolyl endopeptidase	MTELpYDYPK	Y71	1.1	0.9
Q9NZE8	MRPL35	39S ribosomal protein L35, mitochondrial	NWYVDDPpYQK	Y177	1.0	0.9
Q9C0H2	TTYH3	Protein tweety homolog 3	QAHDSLpYR	Y439	1.1	0.7
O43426	SYNJ1	Synaptojanin-1	VTFAPTpYK	Y784	1.0	0.9
Q8IZP0	ABI1	Abl interactor 1	VVAIpYDYTK	Y455	1.1	1.2
Q92499	DDX1	ATP-dependent RNA helicase DDX1	GEpYAVR	Y496	1.1	
Q13131	PRKAA1	5'-AMP-activated protein kinase catalytic subunit alpha-1	VVNPpYYLR	Y441/Y442	1.2	
Q8IZX4	TAF1L	Transcription initiation factor TFIID 210 kDa subunit	YNGPESQpYTK	Y1608	1.1	
Q02218	OGDH	2-oxoglutarate dehydrogenase E1 component, mitochondrial	YHLGMpYHR	Y354	1.2	
Q9BQP7	C20orf72	Uncharacterized protein C20orf72	NQNIQKPEpYSE	Y342	1.2	
P00367	GLUD1	Glutamate dehydrogenase 1, mitochondrial	NLNHVSpYGR	Y451	1.2	
P40763	STAT3	Signal transducer and activator of transcription 3	YCRPESQEHPEADPGSAAPpYLK	Y705	1.4	1.2
P08758	ANXA5	Annexin A5	LYDApYELK	Y94	1.2	
P36959	GMPR	GMP reductase 1	STCTpYVGAAK	Y318	1.3	0.8
P18433	PTPRA	Receptor-type tyrosine-protein phosphatase alpha	VVQEYIDAFSDpYANFK	Y798		0.9
P05771	PRKCB	Protein kinase C beta type	GTDELpYAVK	Y368		0.9
			NLVPMDPNGLSDPpYVK	Y195		0.8
Q5HYK3	COQ5	Ubiquinone biosynthesis methyltransferase COQ5, mitochondrial	SYQpYLVESIR	Y283		1.0
Q01082	SPTBN1	Spectrin beta chain, brain 1	IVSSSDVGHDEpYSTQSLVK	Y777		0.9
P05023	ATP1A1	Sodium/potassium-transporting ATPase subunit alpha-1	GIVVpYTGDR	Y260		0.8
Q9UIQ6	LNPEP	Leucyl-cystinyl aminopeptidase	GLGEHEMEEDEEDpYESSAK	Y70		0.6
Q15126	PMVK	Phosphomevalonate kinase	LLDTSTpYK	Y68		1.0
P17987	TCP1	T-complex protein 1 subunit alpha	HGSpYEDAVHSGALND	Y545		1.2
O14964	HGS	Hepatocyte growth factor-regulated tyrosine kinase substrate	VVQDTpYQIMK	Y132		0.8
Q07912	TNK2	Activated CDC42 kinase 1	KPTpYDPVSEDQDPLSSDFK	Y518		1.0
Q12959	DLG1	Disks large homolog 1	NTSDFVpYLK	Y399		0.6
P05141	ANT2	ADP/ATP translocase 2	AApYFGIYDTAK	Y191		1.0
Q9BRJ2	MRPL45	39S ribosomal protein L45, mitochondrial	FTPPIpYQPK	Y46		0.9
Q96CV9	OPTN	Optineurin	QELVpYTNK	Y356		1.4
Q14162	SCARF1	Endothelial cells scavenger receptor	QAEEERQEEPEpYENVVPISRPPEP	Y818		2.9
Q9UDY2	ZO2	Tight junction protein ZO-2	AYDPDpYER	Y261		1.4
Q99426	TBCB	Tubulin folding cofactor B	LGEpYEDVSR	Y98		0.8
P62805	HIST1H4A	Histone H4	ISGLIpYEETR	Y52		0.9
Q9BU61	C3orf60	Uncharacterized protein C3orf60	LSPADDELpYQR	Y42		1.0

Materials and Methods

Supplementary to: "Targeted Phosphotyrosine Profiling of GPVI Signaling Implicates Oligophrenin-1 in Platelet Filopodia Formation" by Bleijerveld *et al.* (2013*)*

Reagents

Cross-linked collagen related peptide (CRP-XL) and $\alpha_2\beta_1$ binding peptide glycine-phenylalanine-hydroxyproline-glycine-glutamate-arginine (GFOGER) were synthesized and cross-linked as necessary in one of our labs as described [1], but using a CEM Liberty microwave synthesizer. Acetylsalicylic acid was purchased from Sigma; AR-C69931MX was a kind gift from Astra Zeneca. All chemicals used for proteomics experiments were purchased from commercial sources and were of analytical grade. Trypsin (sequencing grade), Complete Mini protease inhibitor and PhosSTOP phosphatase inhibitor cocktails were purchased from Roche Diagnostics; Lys-C was obtained from Wako Chemicals. Microcon YM-30 spin columns were obtained from Millipore; mouse monoclonal anti-phosphotyrosine agarose (PY99, sc-7020) was obtained from Santa Cruz Biotechnology. Adenosine diphosphate (ADP) was purchased from Roche, SFLLRN-trifluoroacetate salt, thrombin receptor activating peptide (TRAP) specific for PAR-1 was purchased from Bachem.

Patients

Although rare, platelets could be obtained from four male Oligophrenin-1 deficient patients. Their legal representatives had given informed consent for drawing blood samples and performing the experiments described in this paper. None of the patients had a history of abnormal haemostasis nor easy bruisability. Moreover, patient 1, a 9 year old boy, underwent several orthodontic and surgical procedures (correction of phymosis, strabism and an adenotomy) without any haemostatic problems. Patients 2 and 3 comprised two affected brothers. The patients had moderate to severe intellectual disability (ID) and in patient 2 and 4 cerebral imaging was performed which revealed vermis hypoplasia and enlarged ventricles. Genetics: Patient 1 showed normal G-banded karyotyping (46) with XY chromosome complement. Array-CGH with the Agilent 105K oligo-array (Oxford design) showed a de novo ~137Kb X:67,249,563-67,386,688(hg18) deletion in Xq12, deleting a large part (exons 6 through 17) of the *OPHN1* gene (total 25 exons). The adult brother pair (patients 2 and 3) had a missense mutation (c.16658A>T;p.Val533Glu) in *OPHN1*. The clinical and molecular characteristics of adult patient 4 have been published previously [2]; he had a loss-of-function mutation (c.556C>T; p.Gln186X) in *OPHN1*. Controls were healthy volunteers.

Blood sample preparation

Venous blood was collected from the patients and healthy volunteers after obtaining informed consent. Blood for mass spectrometry (MS) analysis was collected with an open system, anti-coagulated with 3.2% tri-sodium citrate (Merck). Blood for other experiments was collected using vacuum tubes with 3.2% tri-sodium citrate (BD). Platelet rich plasma (PRP) was prepared by centrifugation of whole blood at 160g for 15 minutes at room temperature, no brake. Washed platelets for mass spectrometry analysis were prepared by adding PRP with ACD (8.5 mM tri-sodium citrate, 7.1 mM citric acid, 5.5 mM D-glucose; final concentration) and centrifugation for 15 minutes with 340g at room temperature, no brake. The platelet pellet was resuspended in Tris-buffer (145 mM NaCl, 5 mM KCl, 260 nM NaH2PO4, 1 mM MgSO4, 100 mM Tris, 5.5 mM D-glucose, pH 6.5) with 10 ng/mL prostacyclin. Platelets were centrifuged for 15 minutes with 340g at room temperature and resuspended up to 200 x 10^9/L in Tris-buffer (pH 7.3), with 100 μM acetylsalicylic acid, and 1 μM AR-C69931MX. Platelets were not used until 30 minutes after isolation. Washed platelets for other experiments were prepared, by adding ACD to PRP and subsequent centrifugation at 340g at room temperature, no brake. The platelet pellet was resuspended in Hepes-Tyrode (HT) buffer (145 mM NaCl, 5mM KCl, 0.5 mM NaH2PO4, 1mM MgSO4, 10 mM Hepes, 5.5 mM D-glucose, pH 6.5) with 10 ng/mL prostacyclin. Platelets were centrifuged for 15 minutes at 340g at

room temperature and resuspended to 200 x 10^9/L in HT-buffer (pH 7.3). Platelets were not used until 30 minutes after isolation.

GPVI stimulation for mass spectrometry analysis
Platelet suspensions were stimulated with 2.5 µg/mL CRP-XL for 5 and 30 minutes. Unstimulated platelet suspensions were taken as control for the same time points. After the indicated incubation times, platelet suspensions were centrifuged at 4000g for 2 minutes, the supernatant aspirated and subsequently the pellet was snap-frozen in liquid nitrogen.

Protein extraction, digestion and stable isotopic labeling of peptides
Mock- or CRP-XL-treated platelet pellets, stored at -80ºC, were rapidly thawed and subsequently lysed on ice in 8M urea in 100 mMTris pH 8.5, 10 mM DTT, 1 mM sodium orthovanadate and 1X PhosSTOP in the presence of protease inhibitors. Efficient lysis was ensured by sonication on ice using a tip sonicator (3 x 30seconds at full power with interval 0.8, followed by 30 seconds continuous sonication) and proteins were further reduced at 56°C for 20 minutes on a shaker (600rpm). Protein concentration was determined using a Bradford Assay (BioRad, Veenendaal, The Netherlands). The total protein lysate from each condition (3 mg total protein) was alkylated with iodoacetamide and subsequently taken for proteolytic digestion using the Filter-Aided Sample Preparation (FASP) procedure (protocol 2), essentially as described in [3]. Lysates were mixed with 0.2 mL of 8 M urea in 0.1 M Tris/HCl pH 8.5 (buffer UA), loaded into Microcon YM30 filtration devices (Millipore), and centrifuged at 14,000g for 15 minutes. The concentrates were diluted in the devices with 0.2 mL of buffer UA and centrifuged again. After centrifugation, the concentrates were mixed with 0.1 mL of 50mM iodoacetamide in UA solution and incubated at room temperature for 30 minutes in the dark. Following centrifugation for 15 minutes, the concentrate was diluted with 0.2mL of UA solution and concentrated again. This step was repeated twice. Next, the concentrate was diluted with 0.1 mL of 8 M urea in 0.1M Tris/HCl pH 8.0 (buffer UB). This step was repeated once. Subsequently, LysC (1:100 w/w) in 30 µL UB was added to the filter and the samples were incubated at 37°C for 4 hours. Then 120 µL ammonium bicarbonate with trypsin (1:50 w/w) was added, followed by overnight incubation at 37°C. The peptides were collected by centrifugation of the filter units, followed by two additional 30 µL filter washes with 0.5M NaCl. Peptides eluted from the FASP-filter unit were desalted and stable isotope dimethyl labeled on a Sep-Pak C18 column (Waters, USA, Massachusetts) as described previously [4, 5]. Control samples were labeled with “light”, and CRP-XL-treated samples with “heavy” label (See Figure 1). For both the 5 minutes and the 30 minutes time point, the light and intermediate sample were mixed in a 1:1 ratio, lyophilized and stored at -80ºC until immunoprecipitation.

Immunoprecipitation (IP) of phosphotyrosine peptides
Immunoprecipitation was performed as described earlier [6-8]. Differentially labeled peptide mixtures of each time point were reconstituted in IP buffer containing 50 mM Tris (pH7.4), 150 mM NaCl, 1% NOG, and protease inhibitor cocktail (Roche diagnostics). Agarose-conjugated anti-p-Tyr (PY99) antibodies (Santa Cruz) (prewashed three times with IP buffer) were added to the peptide mixture and incubated overnight at 4°C under constant rotation. After incubation, the beads were washed three times with 1 ml of IP buffer and twice with 1ml of water, all at 4ºC. Peptides were eluted twice with 0.15% TFA, subsequently desalted and concentrated on stop-and-go extraction (STAGE) tips, dried *in vacuo* and stored at -80ºC until LC-MS analysis.

On-line nanoflow LC-MS
Nanoflow LC-MS/MS was performed by coupling an Agilent 1100 HPLC system (Agilent Technologies, Waldbronn, Germany) to a LTQ-Orbitrap mass spectrometer (Thermo Electron, Bremen, Germany) as described previously [9]. Briefly, dried peptide fractions were reconstituted in 10% formic acid and delivered toa trap column (ReproSil-Pur C18-AQ, 3µm, Dr. Maisch GmbH, Ammerbuch, Germany; 20 mm × 100 µm ID, packed in-house) at 5 µL/min in 100% solvent A (0.1M acetic acid in water).

Subsequently, peptides were transferred to an analytical column (ReproSil-Pur C18-AQ, 3µm, Dr. Maisch GmbH, Ammerbuch, Germany; 40cm × 50 µm ID, packed in-house) at ~100 nL/min in a 3 hour gradient from 0 to 40% solvent B (0.1M acetic acid in 80% Acetonitrile). The mass spectrometer was operated in data dependent mode, automatically switching between MS and MS/MS. Full scan MS spectra (from m/z 300-1500) were acquired in the Orbitrap with a resolution of 60,000 at m/z 400 after accumulation to target value of 500,000. The ten most intense ions at a threshold above 5000 were selected for collision-induced fragmentation in the linear ion trap at normalized collision energy of 35% after accumulation to a target value of 10,000.

Data analysis
All MS2 spectra were converted to single DTA files and mgf files were created using MSQuant 2.0 [10] at default settings. Runs were searched using an in-house licensed MASCOT search engine (Mascot version 2.2) software platform (Matrix Science, London, UK) against the Swissprot human database (version 56.2, 398181 sequences) with carbamidomethyl cysteine as a fixed modification. Light and intermediate dimethylation of peptide N-termini and lysine residues, oxidized methionine and phosphorylation of tyrosine, serine and threonine were set as variable modifications. Trypsin was specified as the proteolytic enzyme and up to one missed cleavage was allowed. The mass tolerance of the precursor ion was set to 5 ppm and for fragment ions to 0.6 Da. The assignment of phosphorylation sites of identified phosphopeptides was performed by the PTM scoring algorithm implemented in MSQuant [10]. Individual MS/MS spectra from phosphopeptides were accepted for a Mascot score ≥ 20. The FDR at this score was estimated to be less than 1% by performing a concatenated decoy database search [6]. All identified phosphopeptides that were found to be differentially phosphorylated were manually scrutinized for site localization. Quantification of peptide doublets was performed using an in-house dimethyl-adapted version of MSQuant [4, 10]. Based on the [CRP-XL/Ctrl] ratio distributions of phosphotyrosine (pTyr) containing and non-phosphorylated peptides, tyrosine phosphorylation was considered significantly regulated over a threshold of 2-fold change (see Figure 2 and Supplementary Figure I B and C). A list of all quantified phosphopeptides is available as Supplementary Table I, and all data are available in the PRIDE database [11] under accession numbers 19671 and 19672: http://tinyurl.com/3cx3ppb.

Western blotting
Washed platelets were lysed in SDS sample buffer (1.1 M glycerol, 62 mM Tris-HCl pH 6.8, 70 mM SDS, 29 µM Broom-phenol blue) and heated at 95°C for 5 minutes. Samples were subjected to SDS-PAGE using a NuPAGE 4%-12% gradient Bis-Tris-HCl pH 6.4 gel (Invitrogen) with MOPS running buffer (Invitrogen) and 50 mM dithiothreitol , electrotransferred to PVDF membrane (Millipore), and immunoblotted with goat anti-human oligophrenin-1 polyclonal antibodies (Santa Cruz), or biotin coupled sheep anti-human GPVI polyclonal antibodies (R&D). Blot was probed with donkey anti-goat IRDye 800CW (LI-COR) and streptavidin IRDye 680 (LI-COR) and imaged using a LI-COR Odyssey imager.

Clot retraction
Citrated PRP was recalcified up to 15 mM $CaCl_2$. Clotting was initiated by adding thrombin up to 0.5 U/mL. Pictures were taken every 3 minutes for 2 hours. Clot surface was manually determined using MacBiophotonics Image J software.

Quantification of platelet membrane proteins
Detection of β_1 receptor was performed with 25 µL APC mouse anti-human CD29 (BD) dissolved in 25µL HEPES buffered saline (HBS; 10 mM HEPES, 150 mMNaCl, 1 mM MgSO4, 5 mM KCl, pH 7.4). Detection of GPIX was performed with 50 uL FITC labeled mouse anti-human CD42a (BD). For GPIb and β3, 2 µL FITC labeled mouse anti-human CD42b (BD), and 2 µL FITC labeled mouse anti-human CD61 (Sanquin) were dissolved in 48 µL HBS, respectively. Labeling was initiated by adding 5 µL fresh, citrate anti-coagulated whole blood to each sample of antibody dilution. After 20 minutes of incubation, the samples were fixed with 500 µL 0.2% formyl saline (0.2% formaldehyde, 0.9% NaCl) and kept at

room temperature until analyses. All samples were analyzed on a FACS Canto II flow cytometer from BD Biosciences on the same day of processing. Single platelets were gated based on forward and side scatter properties. The mean fluorescence intensity (MFI) in the platelet gate was measured with FACS analysis.

Platelet activation and responsiveness
Platelet responsiveness was determined with agonist concentration series for $P2Y_{12}$ (ADP), GPVI (XL-CRP), and PAR-1 (TRAP). Serial dilutions of ADP (125 μM, 31.25 μM, 7.8 μM, 1.95 μM, 488 nM, 122 nM, 31 nM, 8 nM) were prepared in 50 μL, with 2 μL PE labeled mouse anti-human P-selectin (BD) antibodies and 0.5 μL Alexa-488 fibrinogen (Molecular Probes). Similarly serial dilutions of CRP-XL (2.5 μg/mL, 625 ng/mL, 156.3 ng/mL, 39.1 ng/mL, 9.8 ng/mL, 2.4 ng/mL, 600 pg/mL, 153 pg/mL), and TRAP (625 μM, 156.3 μM, 39.1 μM, 9.8 μM, 2.4 μM, 610 nM, 153 nM, 38 nM) were prepared in 50 μL HBS with 2 μL mouse anti-human P-selectin antibodiesand 0.5 μL Alexa-488 fibrinogen. The platelet activation assay was initiated by adding 5 μL fresh, citrate anti-coagulated whole blood to each sample of serial dilutions. Sample incubation, fixation and measurement were performed as described in the 'Quantification of platelet membrane proteins' section. Platelets were defined positive for P-selectin expression or positive for $\alpha_{IIb}\beta_3$ activation when the MFI exceeded 1% of baseline measurement. Non-parametric tests were used to test the difference in response for each concentration of agonist between the patients and healthy controls.

Collagen response under flow.
Cover glasses were coated with collagen dissolved to 100 μg/ml in HBS pH 7.4 for 90 minutes at room temperature. Collagen coated cover glasses were blocked with 1% human serum albumin (HSA; MP Biomedicals) overnight at 4ºC. Whole blood was warmed for 20 minutes at 37ºC, and subsequently perfused at 1600/s over collagen coated cover glasses. Pictures were taken every second for 5 minutes. Pictures were taken using a Zeiss Observer.Z1 microscope coupled to an AxioCamMRm camera and Axiovision Rel. 4.8 software. Platelet surface coverage on collagen was determined automatically with MacBiophotonics Image J software.

Platelet filopodia and lamellipodia formation.
Cover glasses 24 x 60 mm (Mariënfeld) were treated with 2% chromosulfaric acid. Cover glasses were coated with CRP-XL dissolved to 100 μg/ml together with GFOGER dissolved to 100 μg/ml in 10 mM acetic acid, or 100 μg/ml fibrinogen in phosphate buffered saline (PBS: 25 mM Na2HPO4, 2.3 mM NaH2PO4, 140 mM NaCl, pH 7.4) overnight at 4ºC. Coated cover glasses were blocked with 1% HSA for 90 minutes at room temperature. For perfusion with CRP-XL/GFOGER coated coverslips, PRP was added with 0.2 mM RGD. PRP was warmed for 20 minutes at 37ºC, and subsequently perfused at 25/s for 20 minutes. Pictures were taken every 10 seconds with differential interference contrast microscopy (DIC) using a Carl Zeiss Observer Z1 microscope coupled to an AxioCam MRm camera and AxioVision Rel. 4.8 software (Carl Zeiss B.V., Sliedrecht, The Netherlands). For Supplementary Video 1 and 2, frame rates were increased to enhance fluency of the movie. Platelets forming filopodia and lamellipodia were counted and expressed as a percentage of total quantified platelets. Mean filopodia length was determined using Axiovision Rel. 4.8 software using the 'measure length' function. Wilcoxon's rank sum test was used to test the difference between the patients and healthy controls.

References

1. Knight CG, Morton LF, Onley DJ, Peachey AR, Ichinohe T, Okuma M, Farndale RW, Barnes MJ. Collagen-platelet interaction: Gly-pro-hyp is uniquely specific for platelet gp vi and mediates platelet activation by collagen. *Cardiovasc Res*. 1999;41:450-457

2. Kleefstra T, Hamel BC. X-linked mental retardation: Further lumping, splitting and emerging phenotypes. *Clin Genet*. 2005;67:451-467
3. Wisniewski JR, Zougman A, Nagaraj N, Mann M. Universal sample preparation method for proteome analysis. *Nat Methods*. 2009;6:359-362
4. Boersema PJ, Raijmakers R, Lemeer S, Mohammed S, Heck AJ. Multiplex peptide stable isotope dimethyl labeling for quantitative proteomics. *Nat Protoc*. 2009;4:484-494
5. Kovanich D, Cappadona S, Raijmakers R, Mohammed S, Scholten A, Heck AJ. Applications of stable isotope dimethyl labeling in quantitative proteomics. *Anal Bioanal Chem*. 2012; 404(4):991-1009
6. Boersema PJ, Foong LY, Ding VM, Lemeer S, van Breukelen B, Philp R, Boekhorst J, Snel B, den Hertog J, Choo AB, Heck AJ. In-depth qualitative and quantitative profiling of tyrosine phosphorylation using a combination of phosphopeptide immunoaffinity purification and stable isotope dimethyl labeling. *Molecular & cellular proteomics : MCP*. 2010;9:84-99
7. Rikova K, Guo A, Zeng Q, *et al.* Global survey of phosphotyrosine signaling identifies oncogenic kinases in lung cancer. *Cell*. 2007;131:1190-1203
8. Zoumaro-Djayoon AD, Heck AJ, Munoz J. Targeted analysis of tyrosine phosphorylation by immuno-affinity enrichment of tyrosine phosphorylated peptides prior to mass spectrometric analysis. *Methods*. 2012;56:268-274
9. Meiring HD, van der Heeft E, ten Hove GJ, de Jong APJM. Nanoscale lc-ms(n): Technical design and applications to peptide and protein analysis. *J Sep Sci*. 2002;25:557-568
10. Mortensen P, Gouw JW, Olsen JV, Ong SE, Rigbolt KT, Bunkenborg J, Cox J, Foster LJ, Heck AJ, Blagoev B, Andersen JS, Mann M. Msquant, an open source platform for mass spectrometry-based quantitative proteomics. *J Proteome Res*. 2010;9:393-403
11. Vizcaino JA, Cote R, Reisinger F, Barsnes H, Foster JM, Rameseder J, Hermjakob H, Martens L. The proteomics identifications database: 2010 update. *Nucleic Acids Res*. 2010;38:D736-742